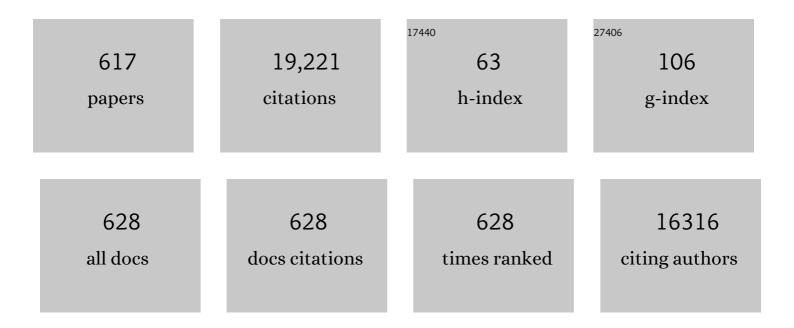
Yoshio Sakka

List of Publications by Year in descending order

Source: https://exaly.com/author-pdf/1608536/publications.pdf Version: 2024-02-01



#	Article	IF	CITATIONS
1	Novel Electronic and Magnetic Properties of Twoâ€Dimensional Transition Metal Carbides and Nitrides. Advanced Functional Materials, 2013, 23, 2185-2192.	14.9	1,418
2	Direct Synthesis of MOFâ€Derived Nanoporous Carbon with Magnetic Co Nanoparticles toward Efficient Water Treatment. Small, 2014, 10, 2096-2107.	10.0	588
3	Electric Double‣ayer Capacitors Based on Highly Graphitized Nanoporous Carbons Derived from ZIFâ€67. Chemistry - A European Journal, 2014, 20, 7895-7900.	3.3	423
4	Two-dimensional molybdenum carbides: potential thermoelectric materials of the MXene family. Physical Chemistry Chemical Physics, 2014, 16, 7841-7849.	2.8	395
5	Electric current activated/assisted sintering (<i>ECAS</i>): a review of patents 1906–2008. Science and Technology of Advanced Materials, 2009, 10, 053001.	6.1	357
6	A high-strain-rate superplastic ceramic. Nature, 2001, 413, 288-291.	27.8	245
7	Dielectrophoretically Aligned Carbon Nanotubes to Control Electrical and Mechanical Properties of Hydrogels to Fabricate Contractile Muscle Myofibers. Advanced Materials, 2013, 25, 4028-4034.	21.0	236
8	Textured Development of Feeble Magnetic Ceramics by Colloidal Processing Under High Magnetic Field. Journal of the Ceramic Society of Japan, 2005, 113, 26-36.	1.3	223
9	Hybrid hydrogels containing vertically aligned carbon nanotubes with anisotropic electrical conductivity for muscle myofiber fabrication. Scientific Reports, 2014, 4, 4271.	3.3	213
10	MOF-derived Nanoporous Carbon as Intracellular Drug Delivery Carriers. Chemistry Letters, 2014, 43, 717-719.	1.3	165
11	Densification behaviour and microstructural development in undoped yttria prepared by flash-sintering. Journal of the European Ceramic Society, 2014, 34, 991-1000.	5.7	159
12	Synthesis and Colloidal Processing of Zirconia Nanopowder. Journal of the American Ceramic Society, 2001, 84, 2489-2494.	3.8	156
13	Textured silicon nitride: processing and anisotropic properties. Science and Technology of Advanced Materials, 2008, 9, 033001.	6.1	142
14	Preparation of porous materials with controlled pore size and porosity. Journal of the European Ceramic Society, 2004, 24, 341-344.	5.7	137
15	Hydrogenâ€Generation Materials for Portable Applications. Journal of the American Ceramic Society, 2008, 91, 3825-3834.	3.8	132
16	Effect of different modification agents on hydrogen-generation by the reaction of Al with water. International Journal of Hydrogen Energy, 2010, 35, 9561-9568.	7.1	128
17	Effect of polyethylenimine on the dispersion and electrophoretic deposition of nano-sized titania aqueous suspensions. Journal of the European Ceramic Society, 2006, 26, 1555-1560.	5.7	124
18	Lowâ€Temperature Processing and Mechanical Properties of Zirconia and Zirconia–Alumina Nanoceramics. Journal of the American Ceramic Society, 2003, 86, 299-304.	3.8	116

#	Article	IF	CITATIONS
19	Trends in electronic structures and structural properties of MAX phases: a first-principles study on M ₂ AlC (M = Sc, Ti, Cr, Zr, Nb, Mo, Hf, or Ta), M ₂ AlN, and hypothetical M ₂ AlB phases. Journal of Physics Condensed Matter, 2014, 26, 505503.	1.8	116
20	Layered Rare-Earth Hydroxides (LRHs) of (Y _{1â^'<i>x</i>} Eu _{<i>x</i>}) ₂ (OH) ₅ NO ₃ · <i>n<!--<br-->(<i>x</i> = 0â^'1): Structural Variations by Eu³⁺ Doping, Phase Conversion to Oxides, and the Correlation of Photoluminescence Behaviors. Chemistry of Materials, 2010, 22, 4204-4213.</i>	i>H ₂	20 114
21	Facile and green production of aqueous graphene dispersions for biomedical applications. Nanoscale, 2015, 7, 6436-6443.	5.6	114
22	High-temperature bending strength, internal friction and stiffness of ZrB2–20vol% SiC ceramics. Journal of the European Ceramic Society, 2012, 32, 2519-2527.	5.7	112
23	Control of Crystal Orientation of Hydroxyapatite by Imposition of a High Magnetic Field. Materials Transactions, 2003, 44, 1133-1137.	1.2	111
24	Modeling of the temperature distribution of flash sintered zirconia. Journal of the Ceramic Society of Japan, 2011, 119, 144-146.	1.1	111
25	Control of texture in alumina by colloidal processing in a strong magnetic field. Science and Technology of Advanced Materials, 2006, 7, 356-364.	6.1	106
26	Flexible Polymer Colloidalâ€Crystal Lasers with a Lightâ€Emitting Planar Defect. Advanced Materials, 2007, 19, 2067-2072.	21.0	106
27	Orientation of mesochannels in continuous mesoporous silica films by a high magnetic field. Journal of Materials Chemistry, 2005, 15, 1137.	6.7	99
28	Dense, bubble-free ceramic deposits from aqueous suspensions by electrophoretic deposition. Journal of Materials Research, 2001, 16, 321-324.	2.6	91
29	Recent progress in advanced optical materials based on gadolinium aluminate garnet (Gd ₃ Al ₅ O ₁₂). Science and Technology of Advanced Materials, 2015, 16, 014902.	6.1	90
30	Fabrication of Macroporous Alumina with Tailored Porosity. Journal of the American Ceramic Society, 2003, 86, 2050-2054.	3.8	89
31	Surface modification of multiwall carbon nanotubes by sulfonitric treatment. Applied Surface Science, 2016, 379, 264-269.	6.1	89
32	Inherent anisotropy in transition metal diborides and microstructure/property tailoring in ultra-high temperature ceramics—A review. Journal of the European Ceramic Society, 2018, 38, 371-389.	5.7	89
33	Spectroscopic study of the discoloration of transparent MgAl2O4 spinel fabricated by spark-plasma-sintering (SPS) processing. Acta Materialia, 2015, 84, 9-19.	7.9	88
34	Greatly enhanced Dy3+ emission via efficient energy transfer in gadolinium aluminate garnet (Gd3Al5O12) stabilized with Lu3+. Journal of Materials Chemistry C, 2013, 1, 7614.	5.5	86
35	Highly Transparent Pure Alumina Fabricated by Highâ€Pressure Spark Plasma Sintering. Journal of the American Ceramic Society, 2010, 93, 2460-2462.	3.8	85
36	Highly textured ZrB2-based ultrahigh temperature ceramics via strong magnetic field alignment. Scripta Materialia, 2009, 60, 615-618.	5.2	84

#	Article	IF	CITATIONS
37	Peculiarities of the neck growth process during initial stage of spark-plasma, microwave and conventional sintering of WC spheres. Journal of Alloys and Compounds, 2012, 523, 1-10.	5.5	82
38	Sizeâ€Tunable UV‣uminescent Silicon Nanocrystals. Small, 2010, 6, 915-921.	10.0	81
39	Highly transparent α-alumina obtained by low cost high pressure SPS. Ceramics International, 2013, 39, 3243-3248.	4.8	81
40	Fabrication of Textured Nb ₄ AlC ₃ Ceramic by Slip Casting in a Strong Magnetic Field and Spark Plasma Sintering. Journal of the American Ceramic Society, 2011, 94, 410-415.	3.8	80
41	Modification of Al Particle Surfaces by gamma-Al2O3 and Its Effect on the Corrosion Behavior of Al. Journal of the American Ceramic Society, 2005, 88, 977-979.	3.8	78
42	The effect of the interlayer element on the exfoliation of layered Mo ₂ AC (A = Al, Si, P, Ga,) Tj ETQq of Advanced Materials, 2014, 15, 014208.	0 0 0 rgBT 6.1	/Overlock 10 78
43	Shell-like nanolayered Nb4AlC3 ceramic with high strength and toughness. Scripta Materialia, 2011, 64, 765-768.	5.2	77
44	Chiroptical Properties Induced in Chiral Photonic-Bandgap Liquid Crystals Leading to a Highly Efficient Laser-Feedback Effect. Advanced Materials, 2006, 18, 775-780.	21.0	76
45	Fabrication of Textured Titania by Slip Casting in a High Magnetic Field Followed by Heating. Japanese Journal of Applied Physics, 2002, 41, L1272-L1274.	1.5	75
46	Electrophoretic Deposition Behavior of Aqueous Nanosized Zinc Oxide Suspensions. Journal of the American Ceramic Society, 2002, 85, 2161-2165.	3.8	74
47	Relation between microstructure, properties and spark plasma sintering (SPS) parameters of pure ultrafine WC powder. Science and Technology of Advanced Materials, 2007, 8, 644-654.	6.1	73
48	Recent advances in understanding the reinforcing ability and mechanism of carbon nanotubes in ceramic matrix composites. Science and Technology of Advanced Materials, 2014, 15, 064902.	6.1	73
49	Nanometer-thin layered hydroxide platelets of (Y0.95Eu0.05)2(OH)5NO3·xH2O: exfoliation-free synthesis, self-assembly, and the derivation of dense oriented oxide films of high transparency and greatly enhanced luminescence. Journal of Materials Chemistry, 2011, 21, 6903.	6.7	72
50	Laser-derived one-pot synthesis of silicon nanocrystals terminated with organic monolayers. Chemical Communications, 2009, , 4684.	4.1	71
51	Thermophysical properties of porous SiC ceramics fabricated by pressureless sintering. Science and Technology of Advanced Materials, 2007, 8, 655-659.	6.1	70
52	Application of constant current pulse to suppress bubble incorporation and control deposit morphology during aqueous electrophoretic deposition (EPD). Journal of the European Ceramic Society, 2009, 29, 1837-1845.	5.7	70
53	Experimental verification of pH localization mechanism of particle consolidation at the electrode/solution interface and its application to pulsed DC electrophoretic deposition (EPD). Journal of the European Ceramic Society, 2010, 30, 1187-1193.	5.7	70
54	Colloidal processing of Gd2O3:Eu3+ red phosphor monospheres of tunable sizes: Solvent effects on precipitation kinetics and photoluminescence properties of the oxides. Acta Materialia, 2011, 59, 3688-3696.	7.9	69

#	Article	IF	CITATIONS
55	Bubbleâ€Free Aqueous Electrophoretic Deposition (EPD) by Pulseâ€Potential Application. Journal of the American Ceramic Society, 2008, 91, 3154-3159.	3.8	68
56	Single-phased luminescent mesoporous nanoparticles for simultaneous cell imaging and anticancer drug delivery. Biomaterials, 2011, 32, 7226-7233.	11.4	68
57	Effect of Ultrasonication on the Microstructure and Tensile Elongation of Zirconiaâ€Dispersed Alumina Ceramics Prepared by Colloidal Processing. Journal of the American Ceramic Society, 2001, 84, 2132-2134.	3.8	67
58	Fabrication of Transparent Yttria by Highâ€Pressure Spark Plasma Sintering. Journal of the American Ceramic Society, 2011, 94, 3206-3210.	3.8	66
59	Size-Dependent Color Tuning of Efficiently Luminescent Germanium Nanoparticles. Langmuir, 2013, 29, 7401-7410.	3.5	66
60	Control of Texture in ZnO by Slip Casting in a Strong Magnetic Field and Heating. Chemistry Letters, 2002, 31, 1204-1205.	1.3	65
61	Preparation of oriented bulk 5wt% Y2O3–AlN ceramics by slip casting in a high magnetic field and sintering. Scripta Materialia, 2005, 52, 583-586.	5.2	65
62	Effects of Pressure Application Method on Transparency of Spark Plasma Sintered Alumina. Journal of the American Ceramic Society, 2011, 94, 1405-1409.	3.8	65
63	Cation Interdiffusion and Phase Stability in Polycrystalline Tetragonal Ceria-Zirconia-Hafnia Solid Solution. Journal of the American Ceramic Society, 1991, 74, 2610-2614.	3.8	64
64	Role of the Initial Degree of Ionization of Polyethylenimine in the Dispersion of Silicon Carbide Nanoparticles. Journal of the American Ceramic Society, 2003, 86, 189-191.	3.8	64
65	Synchrotron X-ray, Photoluminescence, and Quantum Chemistry Studies of Bismuth-Embedded Dehydrated Zeolite Y. Journal of the American Chemical Society, 2012, 134, 2918-2921.	13.7	64
66	Reduction in sintering temperature for flash-sintering of yttria by nickel cation-doping. Acta Materialia, 2016, 106, 344-352.	7.9	64
67	Ultrabroad near-infrared photoluminescence from Bi5(AlCl4)3 crystal. Journal of Materials Chemistry, 2011, 21, 4060.	6.7	63
68	Hybrid White Light Emitting Diode Based on Silicon Nanocrystals. Advanced Functional Materials, 2014, 24, 7151-7160.	14.9	63
69	Luminescent metal nanoclusters: controlled synthesis and functional applications. Science and Technology of Advanced Materials, 2014, 15, 014205.	6.1	63
70	Processing of Silicon Carbide-Mullite-Alumina Nanocomposites. Journal of the American Ceramic Society, 1995, 78, 479-486.	3.8	62
71	Distribution of carbon contamination in oxide ceramics occurring during spark-plasma-sintering (SPS) processing: II - Effect of SPS and loading temperatures. Journal of the European Ceramic Society, 2018, 38, 2596-2604.	5.7	62
72	Magnetically induced orientation of mesochannels in 2D-hexagonal mesoporous silica films. Journal of Materials Chemistry, 2006, 16, 3693.	6.7	61

ΥΟSΗΙΟ SAKKA

#	Article	IF	CITATIONS
73	Microstructure and high-temperature strength of B4C–TiB2 composite prepared by a crucibleless zone melting method. Journal of Alloys and Compounds, 2009, 485, 677-681.	5.5	61
74	Highly Fluorescent Silicaâ€Coated Bismuthâ€Doped Aluminosilicate Nanoparticles for Nearâ€Infrared Bioimaging. Small, 2011, 7, 199-203.	10.0	61
75	Reduced thermal degradation of the red-emitting Sr ₂ Si ₅ N ₈ :Eu ²⁺ phosphor via thermal treatment in nitrogen. Journal of Materials Chemistry C, 2015, 3, 7642-7651.	5.5	60
76	A grain-boundary diffusion model of dynamic grain growth during superplastic deformation. Acta Materialia, 1999, 47, 3433-3439.	7.9	59
77	Transparent nanocrystalline bulk alumina obtained at 7.7GPa and 800°C. Scripta Materialia, 2013, 69, 362-365.	5.2	59
78	Reactive spark plasma sintering of ZrC and HfC ceramics with fine microstructures. Scripta Materialia, 2013, 69, 139-142.	5.2	59
79	Alignment of Titania Whisker by Colloidal Filtration in a High Magnetic Field. Japanese Journal of Applied Physics, 2002, 41, L1416-L1418.	1.5	58
80	The effects of Gd3+ substitution on the crystal structure, site symmetry, and photoluminescence of Y/Eu layered rare-earth hydroxide (LRH) nanoplates. Dalton Transactions, 2012, 41, 1854-1861.	3.3	58
81	In Situ TEM Observation of a Microcrucible Mechanism of Nanowire Growth. Science, 2014, 344, 623-626.	12.6	58
82	A mesoporous non-precious metal boride system: synthesis of mesoporous cobalt boride by strictly controlled chemical reduction. Chemical Science, 2020, 11, 791-796.	7.4	58
83	Tailoring Ti ₃ SiC ₂ Ceramic via a Strong Magnetic Field Alignment Method Followed by Spark Plasma Sintering. Journal of the American Ceramic Society, 2011, 94, 742-748.	3.8	57
84	Effect of sintering temperature on optical properties and microstructure of translucent zirconia prepared by high-pressure spark plasma sintering. Science and Technology of Advanced Materials, 2011, 12, 055003.	6.1	57
85	Magnetically Induced Orientation of Mesochannels in Mesoporous Silica Films at 30â€Tesla. Chemistry - an Asian Journal, 2007, 2, 1505-1512.	3.3	56
86	Photoluminescence, cytotoxicity and in vitro imaging of hexagonal terbium phosphatenanoparticles doped with europium. Nanoscale, 2011, 3, 1263-1269.	5.6	56
87	Highly Concentrated 3D Macrostructure of Individual Carbon Nanotubes in a Ceramic Environment. Advanced Materials, 2012, 24, 4322-4326.	21.0	56
88	Electrophoretic deposition of aqueous nano-Î ³ -Al2O3 suspensions. Materials Research Bulletin, 2002, 37, 653-660.	5.2	55
89	Electrophoretic deposition of alumina suspension in a strong magnetic field. Journal of the European Ceramic Society, 2004, 24, 225-229.	5.7	55
90	Fabrication and some properties of textured alumina-related compounds by colloidal processing in high-magnetic field and sintering. Journal of the European Ceramic Society, 2008, 28, 935-942.	5.7	55

#	Article	IF	CITATIONS
91	Dense zircon (ZrSiO4) ceramics by high energy ball milling and spark plasma sintering. Ceramics International, 2012, 38, 1793-1799.	4.8	55
92	Fluorescent sensing of colloidal CePO ₄ :Tb nanorods for rapid, ultrasensitive and selective detection of vitamin C. Nanotechnology, 2010, 21, 365501.	2.6	53
93	The development of Ce ³⁺ -activated (Gd,Lu) ₃ Al ₅ O ₁₂ garnet solid solutions as efficient yellow-emitting phosphors. Science and Technology of Advanced Materials, 2013, 14, 054201.	6.1	53
94	A strategy for fabricating textured silicon nitride with enhanced thermal conductivity. Journal of the European Ceramic Society, 2014, 34, 2585-2589.	5.7	53
95	Influence of microstructure on the thermophysical properties of sintered SiC ceramics. Journal of Alloys and Compounds, 2008, 463, 493-497.	5.5	52
96	High-temperature reactive spark plasma consolidation of TiB2–NbC ceramic composites. Ceramics International, 2015, 41, 10828-10834.	4.8	52
97	Ultrabroad near-infrared photoluminescence from ionic liquids containing subvalent bismuth. Optics Letters, 2011, 36, 100.	3.3	51
98	Doped-carbon electrocatalysts with trimodal porosity from a homogeneous polypeptide gel. Journal of Materials Chemistry A, 2013, 1, 13576.	10.3	51
99	Ultra-high elevated temperature strength of TiB2-based ceramics consolidated by spark plasma sintering. Journal of the European Ceramic Society, 2017, 37, 393-397.	5.7	51
100	Superconducting and Transport Properties of B-Y-Cu-O Compounds -Orthorhombic and Tetragonal Phases. Japanese Journal of Applied Physics, 1987, 26, L721-L723.	1.5	50
101	Physical and mechanical properties of highly textured polycrystalline Nb ₄ AlC ₃ ceramic. Science and Technology of Advanced Materials, 2011, 12, 044603.	6.1	50
102	Strong <scp><scp>ZrB</scp></scp> ₂ – <scp><scp>SiC</scp>–<scp><scp>WC</scp></scp> Ceramics at 1600°C. Journal of the American Ceramic Society, 2012, 95, 874-878.</scp>	3.8	50
103	Layered rare-earth hydroxide and oxide nanoplates of the Y/Tb/Eu system: phase-controlled processing, structure characterization and color-tunable photoluminescence via selective excitation and efficient energy transfer. Science and Technology of Advanced Materials, 2013, 14, 015006.	6.1	50
104	One-step freezing temperature crystallization of layered rare-earth hydroxide (Ln ₂ (OH) ₅ NO ₃ ·nH ₂ O) nanosheets for a wide spectrum of Ln (Ln = Pr–Er, and Y), anion exchange with fluorine and sulfate, and microscopic coordination probed via photoluminescence. Journal of Materials Chemistry C, 2015, 3, 3428-3437.	5.5	50
105	Auto-programmed synthesis of metallic aerogels: Core-shell Cu@Fe@Ni aerogels for efficient oxygen evolution reaction. Nano Energy, 2021, 81, 105644.	16.0	50
106	Fabrication of porous ceramics with controlled pore size by colloidal processing. Science and Technology of Advanced Materials, 2005, 6, 915-920.	6.1	49
107	Control of crystalline texture in polycrystalline TiO2 (Anatase) by electrophoretic deposition in a strong magnetic field. Journal of the European Ceramic Society, 2006, 26, 559-563.	5.7	49
108	Experimental and theoretical studies of photoluminescence from Bi82+ and Bi53+ stabilized by [AlCl4]â^' in molecular crystals. Journal of Materials Chemistry, 2012, 22, 12837.	6.7	49

#	Article	IF	CITATIONS
109	Influence of pre- and post-annealing on discoloration of MgAl2O4 spinel fabricated by spark-plasma-sintering (SPS). Journal of the European Ceramic Society, 2016, 36, 2961-2968.	5.7	49
110	Superplasticity in alumina enhanced by co-dispersion of 10% zirconia and 10% spinel particles. Acta Materialia, 2001, 49, 887-895.	7.9	48
111	High-pressure spark plasma sintering of MgO-doped transparent alumina. Journal of the Ceramic Society of Japan, 2012, 120, 116-118.	1.1	48
112	High-strength TiB 2 –TaC ceramic composites prepared using reactive spark plasma consolidation. Ceramics International, 2016, 42, 1298-1306.	4.8	48
113	Enhanced superplasticity in a alumina-containing zirconia prepared by colloidal processing. Scripta Materialia, 2000, 43, 705-710.	5.2	47
114	Nonisothermal Synthesis of Yttriaâ€Stabilized Zirconia Nanopowder through Oxalate Processing: I, Characteristics of Yâ€Zr Oxalate Synthesis and Its Decomposition. Journal of the American Ceramic Society, 2000, 83, 2196-2202.	3.8	47
115	High-hardness B4C textured by a strong magnetic field technique. Scripta Materialia, 2011, 64, 256-259.	5.2	47
116	Reaction temperature variations on the crystallographic state of spinel cobalt aluminate. Dalton Transactions, 2013, 42, 7167.	3.3	47
117	Electrophoretic deposition of aqueous nano-sized zinc oxide suspensions on a zinc electrode. Materials Research Bulletin, 2003, 38, 207-212.	5.2	46
118	Effect of Polyethylenimine on Hydrolysis and Dispersion Properties of Aqueous Si3N4Suspensions. Journal of the American Ceramic Society, 2007, 90, 797-804.	3.8	46
119	Zircon–zirconia (ZrSiO4–ZrO2) dense ceramic composites by spark plasma sintering. Journal of the European Ceramic Society, 2012, 32, 787-793.	5.7	46
120	One-pot synthesis of monoclinic ZrO2 nanocrystals under subcritical hydrothermal conditions. Journal of Supercritical Fluids, 2014, 85, 57-61.	3.2	46
121	Flash spark plasma sintering of ultrafine yttria-stabilized zirconia ceramics. Scripta Materialia, 2016, 121, 32-36.	5.2	46
122	Amorphous Alloy Architectures in Pore Walls: Mesoporous Amorphous NiCoB Alloy Spheres with Controlled Compositions <i>via</i> a Chemical Reduction. ACS Nano, 2020, 14, 17224-17232.	14.6	46
123	Tri-axial Grain Orientation of Y ₂ Ba ₄ Cu ₇ O _{<i>y</i>} Achieved by the Magneto-science Method. Applied Physics Express, 0, 1, 111701.	2.4	46
124	Dispersion Behavior of ZrB2Powder in Aqueous Solution. Journal of the American Ceramic Society, 2007, 90, 3455-3459.	3.8	45
125	Pressure Effects on Temperature Distribution during Spark Plasma Sintering with Graphite Sample. Materials Transactions, 2009, 50, 2111-2114.	1.2	45
126	Gelcasting of alumina with a new monomer synthesized from glucose. Journal of the European Ceramic Society, 2010, 30, 1795-1801.	5.7	44

#	Article	IF	CITATIONS
127	Effect of sintering conditions on microstructure orientation in α-SiC prepared by slip casting in a strong magnetic field. Journal of the European Ceramic Society, 2010, 30, 2813-2817.	5.7	44
128	Influence of Spark Plasma Sintering (<scp>SPS</scp>) Conditions on Transmission of MgAl ₂ O ₄ Spinel. Journal of the American Ceramic Society, 2015, 98, 378-385.	3.8	44
129	Microstructure and properties of ZrB2–SiC composites prepared by spark plasma sintering using TaSi2 as sintering additive. Journal of the European Ceramic Society, 2010, 30, 2625-2631.	5.7	43
130	Effective lattice stabilization of gadolinium aluminate garnet (GdAG) via Lu ³⁺ doping and development of highly efficient (Gd,Lu)AG:Eu ³⁺ red phosphors. Science and Technology of Advanced Materials, 2012, 13, 035007.	6.1	43
131	Microstructure and high-temperature strength of textured and non-textured ZrB ₂ ceramics. Science and Technology of Advanced Materials, 2014, 15, 014202.	6.1	43
132	Distribution of carbon contamination in MgAl2O4 spinel occurring during spark-plasma-sintering (SPS) processing: I – Effect of heating rate and post-annealing. Journal of the European Ceramic Society, 2018, 38, 2588-2595.	5.7	43
133	Processing and properties of sintered reaction-bonded silicon nitride with Y2O3–MgSiN2: Effects of Si powder and Li2O addition. Acta Materialia, 2007, 55, 5581-5591.	7.9	42
134	Tens of micron-sized unilamellar nanosheets of Y/Eu layered rare-earth hydroxide: efficient exfoliation via fast anion exchange and their self-assembly into oriented oxide film with enhanced photoluminescence. Science and Technology of Advanced Materials, 2014, 15, 014203.	6.1	42
135	High-strain-rate superplasticity in oxide ceramics. Science and Technology of Advanced Materials, 2007, 8, 578-587.	6.1	41
136	Interfacial-related color tuning of colloidal Si nanocrystals. Green Chemistry, 2010, 12, 2139.	9.0	41
137	Effect of Alumina Dopant on Transparency of Tetragonal Zirconia. Journal of Nanomaterials, 2012, 2012, 1-5.	2.7	41
138	Compressive deformation of CoZr and (Co,Ni)Zr intermetallic compounds with B2 structure. Journal of Materials Science, 1988, 23, 4041-4048.	3.7	40
139	Preferred Orientation of the Texture in the SiC Whisker-Dispersed Al2O3 Ceramics by Slip Casting in a High Magnetic Field Journal of the Ceramic Society of Japan, 2001, 109, 886-890.	1.3	40
140	Texture Development in Si3N4 Ceramics by Magnetic Field Alignment during Slip Casting. Journal of the Ceramic Society of Japan, 2006, 114, 979-987.	1.3	40
141	Hardness and Fracture Toughness of Alumina-Doped Tetragonal Zirconia with Different Yttria Contents. Materials Transactions, 2003, 44, 2235-2238.	1.2	39
142	Textured HfB2-based ultrahigh-temperature ceramics with anisotropic oxidation behavior. Scripta Materialia, 2009, 60, 913-916.	5.2	39
143	Low temperature thermal expansion, high temperature electrical conductivity, and mechanical properties of Nb4AlC3 ceramic synthesized by spark plasma sintering. Journal of Alloys and Compounds, 2009, 487, 675-681.	5.5	39
144	Well-defined crystallites autoclaved from the nitrate/NH4OH reaction system as the precursor for (Y,Eu)2O3 red phosphor: Crystallization mechanism, phase and morphology control, and luminescent property. Journal of Solid State Chemistry, 2012, 192, 229-237.	2.9	39

#	Article	IF	CITATIONS
145	Machinable ZrB2–SiC–BN composites fabricated by reactive spark plasma sintering. Materials Science & Engineering A: Structural Materials: Properties, Microstructure and Processing, 2013, 582, 41-46.	5.6	39
146	Fabrication of high-strain rate superplastic yttria-doped zirconia polycrystals by adding manganese and aluminum oxides. Journal of the European Ceramic Society, 2004, 24, 449-453.	5.7	38
147	Lowâ€Temperature Spark Plasma Sintering of Pure Nano <scp>WC</scp> Powder. Journal of the American Ceramic Society, 2013, 96, 1702-1705.	3.8	38
148	Oxidation and Degradation of Titanium Nitride Ultrafine Powders Exposed to Air. Journal of the American Ceramic Society, 1992, 75, 244-248.	3.8	37
149	Electrophoretic deposition of lead zirconate titanate (PZT) powder from ethanol suspension prepared with phosphate ester. Science and Technology of Advanced Materials, 2005, 6, 927-932.	6.1	37
150	Effect of loading schedule on densification of MgAl2O4 spinel during spark plasma sintering (SPS) processing. Journal of the European Ceramic Society, 2012, 32, 2303-2309.	5.7	37
151	Unprecedented simultaneous enhancement in strain tolerance, toughness and strength of Al ₂ O ₃ ceramic by multiwall-type failure of a high loading of carbon nanotubes. Nanotechnology, 2013, 24, 155702.	2.6	37
152	Assessment of carbon contamination in MgAl ₂ O ₄ spinel during spark-plasma-sintering (SPS) processing. Journal of the Ceramic Society of Japan, 2015, 123, 983-988.	1.1	37
153	Densification, microstructure evolution and mechanical properties of WC doped HfB2–SiC ceramics. Journal of the European Ceramic Society, 2015, 35, 2707-2714.	5.7	37
154	Transparent ultrafine Yb ³⁺ :Y ₂ O ₃ laser ceramics fabricated by spark plasma sintering. Journal of the American Ceramic Society, 2018, 101, 694-702.	3.8	37
155	High‣trainâ€Rate Superplasticity in Y ₂ 0 ₃ ‣tabilized Tetragonal ZrO ₂ Dispersed with 30 vol% MgAl ₂ O ₄ Spinel. Journal of the American Ceramic Society, 2002, 85, 1900-1902.	3.8	36
156	Pressure Effect on the Homogeneity of Spark Plasma‧intered Tungsten Carbide Powder. Journal of the American Ceramic Society, 2009, 92, 2418-2421.	3.8	36
157	Hydrogen generation from water using Mg nanopowder produced by arc plasma method. Science and Technology of Advanced Materials, 2012, 13, 025009.	6.1	36
158	Structure characterization and photoluminescence properties of (Y0.95â^'xGdxEu0.05)2O3 red phosphors converted from layered rare-earth hydroxide (LRH) nanoflake precursors. Journal of Alloys and Compounds, 2013, 559, 188-195.	5.5	36
159	Dynamic grain growth during low-temperature spark plasma sintering of alumina. Scripta Materialia, 2014, 80, 29-32.	5.2	36
160	Prevention of thermal- and moisture-induced degradation of the photoluminescence properties of the Sr ₂ Si ₅ N ₈ :Eu ²⁺ red phosphor by thermal post-treatment in N ₂ –H ₂ . Physical Chemistry Chemical Physics, 2016, 18, 12494-12504.	2.8	36
161	Magnetic orientation and magnetic anisotropy in paramagnetic layered oxides containing rare-earth ions. Science and Technology of Advanced Materials, 2009, 10, 014604.	6.1	35
162	NMR, ESR, and Luminescence Characterization of Bismuth Embedded Zeolites Y. Journal of Physical Chemistry C, 2013, 117, 6399-6408.	3.1	35

#	Article	IF	CITATIONS
163	Synthesis of B ₆ O powder and spark plasma sintering of B ₆ O and B ₆ O–B ₄ C ceramics. Journal of the Ceramic Society of Japan, 2013, 121, 950-955.	1.1	35
164	Hydroxide synthesis, colloidal processing and sintering of nano-size 3Y-TZP powder. Scripta Materialia, 2001, 44, 2219-2223.	5.2	34
165	Potential use of only Yb ₂ O ₃ in producing dense Si ₃ N ₄ ceramics with high thermal conductivity by gas pressure sintering. Science and Technology of Advanced Materials, 2010, 11, 065001.	6.1	34
166	Development of Eu3+ activated monoclinic, perovskite, and garnet compounds in the Gd2O3–Al2O3 phase diagram as efficient red-emitting phosphors. Journal of Solid State Chemistry, 2013, 206, 104-112.	2.9	34
167	Toughness control of boron carbide obtained by spark plasma sintering in nitrogen atmosphere. Ceramics International, 2014, 40, 3053-3061.	4.8	34
168	Effect of texture on oxidation resistance of Ti3AlC2. Journal of the European Ceramic Society, 2018, 38, 3417-3423.	5.7	34
169	Preparation Methods and Superplastic Properties of Fine-Grained Zirconia and Alumina Based Ceramics Nippon Kagaku Kaishi / Chemical Society of Japan - Chemistry and Industrial Chemistry Journal, 1999, 1999, 497-508.	0.1	33
170	Circularly Polarized Laser Emission Induced by Supramolecular Chirality in Cholesteric Liquid Crystals. Journal of Nanoscience and Nanotechnology, 2006, 6, 1819-1822.	0.9	33
171	Effect of sintering additive on crystallographic orientation in AlN prepared by slip casting in a strong magnetic field. Journal of the European Ceramic Society, 2009, 29, 2627-2633.	5.7	33
172	Transparent magneto-optical Ho2O3 ceramics: Role of self-reactive resultant oxyfluoride additive and investigation of vacuum sintering kinetics. Ceramics International, 2019, 45, 14761-14767.	4.8	33
173	Fabrication of oriented ?-alumina from porous bodies by slip casting in a high magnetic field. Solid State Ionics, 2004, 172, 341-347.	2.7	32
174	Effect of pH localization on microstructure evolution of deposits during aqueous electrophoretic deposition (EPD). Journal of the European Ceramic Society, 2010, 30, 2467-2473.	5.7	32
175	Textured h-BN Ceramics Prepared by Slip Casting. Journal of the American Ceramic Society, 2011, 94, 1397-1404.	3.8	32
176	Ultra-broad near-infrared photoluminescence from crystalline (K-crypt)2Bi2 containing [Bi2]2â^' dimers. Journal of Materials Chemistry, 2012, 22, 20175.	6.7	32
177	Microstructure characterization of ZrB2–SiC composite fabricated by spark plasma sintering with TaSi2 additive. Journal of the European Ceramic Society, 2012, 32, 1441-1446.	5.7	32
178	Synthesis of Highâ€Purity Ti ₃ SiC ₂ by Microwave Sintering. International Journal of Applied Ceramic Technology, 2014, 11, 911-918.	2.1	32
179	Controlled Synthesis of Layered Rareâ€Earth Hydroxide Nanosheets Leading to Highly Transparent (Y _{0.95} Eu _{0.05}) ₂ O ₃ Ceramics. Journal of the American Ceramic Society, 2015, 98, 1413-1422.	3.8	32
180	Photocatalytic growth of Ag nanocrystals on hydrothermally synthesized multiphasic TiO2/reduced graphene oxide (rGO) nanocomposites and their SERS performance. Applied Surface Science, 2017, 423, 1-12.	6.1	32

#	Article	IF	CITATIONS
181	Nonisothermal Synthesis of Yttria‧tabilized Zirconia Nanopowder through Oxalate Processing: II, Morphology Manipulation. Journal of the American Ceramic Society, 2001, 84, 2484-2488.	3.8	31
182	Microstructure and properties of ZrB2-SiC and HfB2-SiC composites fabricated by spark plasma sintering (SPS) using TaSi2 as sintering aid. Journal of the Ceramic Society of Japan, 2010, 118, 997-1001.	1.1	31
183	Forming and Microstructure Control of Ceramics by Electrophoretic Deposition (EPD). KONA Powder and Particle Journal, 2010, 28, 74-90.	1.7	31
184	Effects of Gd Substitution on Sintering and Optical Properties of Highly Transparent (Y _{0.95â^'<i>x</i>} Gd _{<i>x</i>} Eu _{0.05}) ₂ O ₃ Ceramics. Journal of the American Ceramic Society, 2015, 98, 2480-2487.	3.8	31
185	Hydrothermal crystallization of a Ln ₂ (OH) ₄ SO ₄ ·nH ₂ O layered compound for a wide range of Ln (Ln = Laâ \in 'Dy), thermolysis, and facile transformation into oxysulfate and oxysulfide phosphors. RSC Advances, 2017, 7, 13331-13339.	3.6	31
186	Nanoexplosion Synthesis of Multimetal Oxide Ceramic Nanopowders. Nano Letters, 2005, 5, 2598-2604.	9.1	30
187	Mechanical properties of textured, multilayered alumina produced using electrophoretic deposition in a strong magnetic field. Journal of the European Ceramic Society, 2006, 26, 661-665.	5.7	30
188	Fabrication of multilayered oxide thermoelectric modules by electrophoretic deposition under high magnetic fields. Applied Physics Letters, 2006, 89, 081912.	3.3	30
189	Effect of starting powders on the sintering of nanostructured ZrO2ceramics by colloidal processing. Science and Technology of Advanced Materials, 2009, 10, 025004.	6.1	30
190	Synthesis of Plate‣ike <scp><scp>ZrB₂</scp></scp> Grains. Journal of the American Ceramic Society, 2012, 95, 85-88.	3.8	30
191	Efficient green-luminescent germanium nanocrystals. Journal of Materials Chemistry A, 2013, 1, 3747.	10.3	30
192	Controlled processing of (Gd,Ln) ₂ O ₃ :Eu (Ln = Y, Lu) red phosphor particles and compositional effects on photoluminescence. Science and Technology of Advanced Materials, 2013, 14, 064202.	6.1	30
193	Electrophoretic deposition of α-alumina particles in a strong magnetic field. Journal of Materials Research, 2003, 18, 254-256.	2.6	29
194	Gadolinium Aluminate Garnet (<scp><scp>Gd₃Al₅O₁₂</scp></scp>): Crystal Structure Stabilization via Lutetium Doping and Properties of the (<scp><scp>Gd</scp></scp> _{1â[°]<i>x</i>} <scp><scp>Lu</scp></scp> _{<i>x</i>}) _{3 Solid Solutions (<i>xÂ</i>}): Journal of the American Ceramic Society, 2012, 95, 931-936.	3.8 <sc < td=""><td>29 p><scp>Al<s< td=""></s<></scp></td></sc <>	29 p> <scp>Al<s< td=""></s<></scp>
195	a€ ⁻ Beautifulâ€ [™] unconventional synthesis and processing technologies of superconductors and some other materials. Science and Technology of Advanced Materials, 2011, 12, 013001.	6.1	29
196	Study of phase transformation behaviour of alumina through precipitation method. Journal Physics D: Applied Physics, 2012, 45, 215302.	2.8	29
197	Photoluminescence from Bi5(GaCl4)3 molecular crystal. Dalton Transactions, 2012, 41, 11055.	3.3	29
198	Transparent hydroxyapatite ceramics consolidated by spark plasma sintering. Scripta Materialia, 2013, 69, 366-369.	5.2	29

#	Article	IF	CITATIONS
199	<i>>In Situ</i> Fabrication of <scp><scp>B</scp></scp> ₄ <scp>C</scp> a€" <scp>NbB</scp> 2Eutectic Composites by Sparkâ€"Plasma Sintering. Journal of the American Ceramic Society, 2014, 97, 2376-2378.	b _{}.8}	29
200	Densification and Cell Performance of Gadolinium-Doped Ceria (GDC) Electrolyte/NiO-GDC Anode Laminates. Journal of the American Ceramic Society, 2009, 92, S117-S121.	3.8	28
201	Micro-emulsion synthesis of blue-luminescent silicon nanoparticles stabilized with alkoxy monolayers. Journal of Crystal Growth, 2009, 311, 634-637.	1.5	28
202	Surface modification of Ca-α-SiAlON: Eu2+ phosphor particles by SiO2 coating and fabrication of its deposit by electrophoretic deposition (EPD) process. Applied Surface Science, 2013, 280, 229-234.	6.1	28
203	Texture development of hydroxyapatite ceramics by colloidal processing in a high magnetic field followed by sintering. Materials Science & Engineering A: Structural Materials: Properties, Microstructure and Processing, 2008, 475, 27-33.	5.6	27
204	Effect of alumina addition on initial sintering of cubic ZrO2 (8YSZ). Ceramics International, 2010, 36, 879-885.	4.8	27
205	Highly Infrared Transparent Nanometric Tetragonal Zirconia Prepared by Highâ€Pressure Spark Plasma Sintering. Journal of the American Ceramic Society, 2011, 94, 2739-2741.	3.8	27
206	Electrophoretic Deposition of <scp><scp>Ti</scp></scp> ₃ <scp><scp>SiC</scp>₂ and Texture Development in a Strong Magnetic Field. Journal of the American Ceramic Society, 2012, 95, 2857-2862.</scp>	3.8	27
207	Spark Plasma Sintering of Diamond Binderless <scp>WC</scp> Composites. Journal of the American Ceramic Society, 2012, 95, 2423-2428.	3.8	27
208	Thermal Conversion of Hollow Prussian Blue Nanoparticles into Nanoporous Iron Oxides with Crystallized Hematite Phase. European Journal of Inorganic Chemistry, 2014, 2014, 1137-1141.	2.0	27
209	Reactive spark plasma sintering of binderless WC ceramics at 1500°C. International Journal of Refractory Metals and Hard Materials, 2014, 43, 42-45.	3.8	27
210	Low-temperature sintering and gas desorption of gold ultrafine powders. Journal of the Less Common Metals, 1989, 147, 89-96.	0.8	26
211	Nano-engineering of zirconia–noble metals composites. Journal of the European Ceramic Society, 2004, 24, 469-473.	5.7	26
212	Densification and Superplasticity of Hydroxyapatite Ceramics. Journal of the Ceramic Society of Japan, 2005, 113, 669-673.	1.3	26
213	Conductive Polymer Coating on Nonconductive Ceramic Substrates for Use in the Electrophoretic Deposition Process. Journal of the American Ceramic Society, 2008, 91, 1674-1677.	3.8	26
214	Corrosion of ZrB ₂ Powder During Wet Processing – Analysis and Control. Journal of the American Ceramic Society, 2008, 91, 1715-1717.	3.8	26
215	Formation of zirconia films by the aerosol gas deposition method. Journal of the Ceramic Society of Japan, 2010, 118, 767-770.	1.1	26
216	Grain boundary diffusion driven spark plasma sintering of nanocrystalline zirconia. Ceramics International, 2012, 38, 4385-4389.	4.8	26

#	Article	IF	CITATIONS
217	45S5 Bioglass®–MWCNT composite: processing and bioactivity. Journal of Materials Science: Materials in Medicine, 2015, 26, 199.	3.6	26
218	Cation Interdiffusion in Polycrystalline Fluorite-cubic MgO–ZrO2Solid Solution. Bulletin of the Chemical Society of Japan, 1982, 55, 420-422.	3.2	25
219	Effect of Ultrasonication on Colloidal Dispersion of Al ₂ O ₃ and ZrO ₂ Powders in pH Controlled Suspension. Materials Transactions, JIM, 1998, 39, 689-692.	0.9	25
220	Processingâ€Dependent Microstructural Factors Affecting Cavitation Damage and Tensile Ductility in a Superplastic Alumina Dispersed with Zirconia. Journal of the American Ceramic Society, 2002, 85, 2763-2770.	3.8	25
221	Preparation of Crystallineâ€Oriented Titania Photoelectrodes on ITO Glasses from a 2â€Propanol–2,4â€Pentanedione Solvent by Electrophoretic Deposition in a Strong Magnetic Field. Journal of the American Ceramic Society, 2009, 92, 984-989.	3.8	25
222	Role of Particle Sizes in Hydrogen Generation by the Reaction of Al with Water. Journal of the American Ceramic Society, 2010, 93, 2998-3001.	3.8	25
223	Microstructure and mechanical properties of ZrB2–SiC–BN composites fabricated by reactive hot pressing and reactive spark plasma sintering. Scripta Materialia, 2013, 68, 889-892.	5.2	25
224	Research progress in nondoped lanthanoid silicate oxyapatites as new oxygen-ion conductors. Journal of the Ceramic Society of Japan, 2014, 122, 921-939.	1.1	25
225	Tough and dense boron carbide obtained by high-pressure (300 MPa) and low-temperature (1600°C) spark plasma sintering. Journal of the Ceramic Society of Japan, 2014, 122, 271-275.	1.1	25
226	Effect of texture microstructure on tribological properties of tailored Ti3AlC2 ceramic. Journal of Advanced Ceramics, 2017, 6, 120-128.	17.4	25
227	Effect of MgSiN2 addition on gas pressure sintering and thermal conductivity of silicon nitride with Y2O3. Journal of the Ceramic Society of Japan, 2008, 116, 706-711.	1.1	24
228	Spectroscopic characterization of bismuth embedded Y zeolites. Applied Physics Letters, 2010, 97, .	3.3	24
229	Thermal conductivity of EB-PVD ZrO2–4mol% Y2O3 films using the laser flash method. Journal of Alloys and Compounds, 2011, 509, 1045-1049.	5.5	24
230	Monodisperse colloidal spheres for (Y,Eu)2O3red-emitting phosphors: establishment of processing window and size-dependent luminescence behavior. Science and Technology of Advanced Materials, 2011, 12, 055001.	6.1	24
231	High Hardness B _{<i>a</i>} C _{<i>b</i>} -(B _{<i>x</i>} O _{<i>y</i>} /BN) Composites with 3D Mesh-Like Fine Grain-Boundary Structure by Reactive Spark Plasma Sintering. Journal of Nanoscience and Nanotechnology, 2012, 12, 959-965.	0.9	24
232	Fluorescent and paramagnetic core–shell hybrid nanoparticles for bi-modal magnetic resonance/luminescence imaging. Journal of Materials Chemistry, 2012, 22, 20641.	6.7	24
233	Effective Use of Mesoporous Silica Filler: Comparative Study on Thermal Stability and Transparency of Silicone Rubbers Loaded with Various Kinds of Silica Particles. European Journal of Inorganic Chemistry, 2014, 2014, 2773-2778.	2.0	24
234	Pressureless Sintering and Reaction Mechanisms of <scp><scp>Ti</scp></scp> 3 <scp>SiC</scp> 2 Ceramics. Journal of the American Ceramic Society, 2014, 97, 1407-1412.	3.8	24

#	Article	IF	CITATIONS
235	Highâ€Strength B ₄ C–TaB ₂ Eutectic Composites Obtained via <i>In Situ</i> by Spark Plasma Sintering. Journal of the American Ceramic Society, 2016, 99, 2436-2441.	3.8	24
236	Preparation and Some Electrical Properties of Yttrium-Doped Antimonic Acids. Chemistry of Materials, 2003, 15, 928-934.	6.7	23
237	Fabrication of Highly Microstructure Controlled Ceramics by Novel Colloidal Processing. Journal of the Ceramic Society of Japan, 2006, 114, 371-376.	1.3	23
238	An efficient and biocompatible fluorescence resonance energy transfer system based on lanthanide-doped nanoparticles. Nanotechnology, 2010, 21, 455703.	2.6	23
239	Synthesis, microstructure and mechanical properties of (Zr,Ti)B2-(Zr,Ti)N composites prepared by spark plasma sintering. Journal of Alloys and Compounds, 2010, 494, 266-270.	5.5	23
240	pH localization: a case study during electrophoretic deposition of ternary MAX phase carbide-Ti ₃ SiC ₂ . Journal of the Ceramic Society of Japan, 2013, 121, 348-354.	1.1	23
241	Fabrication of textured Ti ₃ AlC ₂ by spark plasma sintering and their anisotropic mechanical properties. Journal of the Ceramic Society of Japan, 2013, 121, 366-369.	1.1	23
242	Facile and green synthesis of (La _{0.95} Eu _{0.05}) ₂ O ₂ S red phosphors with sulfate-ion pillared layered hydroxides as a new type of precursor: controlled hydrothermal processing, phase evolution and photoluminescence. Science and Technology of Advanced Materials, 2014, 15, 014204.	6.1	23
243	Transparent ZnAl ₂ O ₄ ceramics fabricated by spark plasma sintering. Journal of the Ceramic Society of Japan, 2014, 122, 784-787.	1.1	23
244	Rietveld Texture Analysis of Alumina Ceramics by Neutron Diffraction. Chemistry of Materials, 2005, 17, 102-106.	6.7	22
245	Texture Development in Alumina Composites by Slip Casting in a Strong Magnetic Field. Journal of the Ceramic Society of Japan, 2006, 114, 59-62.	1.3	22
246	Fabrication of Hierarchically Porous Spherical Particles by Assembling Mesoporous Silica Nanoparticles via Spray Drying. Journal of Nanoscience and Nanotechnology, 2008, 8, 3101-3105.	0.9	22
247	Rare-Earth-Dependent Magnetic Anisotropy in REBa ₂ Cu ₃ O _{<i>y</i>} . Applied Physics Express, 0, 1, 031701.	2.4	22
248	Formation of zirconia films by aerosol gas deposition method using zirconia powder produced by break-down method. Journal of the Ceramic Society of Japan, 2010, 118, 948-951.	1.1	22
249	Rudimental research progress of rare-earth silicate oxyapatites: their identification as a new compound until discovery of their oxygen ion conductivity. Journal of the Ceramic Society of Japan, 2014, 122, 649-663.	1.1	22
250	Microstructure and <scp>A</scp> nisotropic <scp>P</scp> roperties of <scp>T</scp> extured <scp>Z</scp> r <scp>B</scp> ₂ and <scp>Z</scp> r <scp>B</scp> ₂ â€" <scp>M</scp> o <scp>S</scp> i ₂ Â <scp>C</scp> erami <scp>P</scp> repared by <scp>S</scp> trong <scp>M</scp> agnetic <scp>F</scp> ield <scp>A</scp> lignment. International Journal of Applied Ceramic Technology, 2014, 11, 218-227.	C 2. 1	22
251	Sintering characteristics and thermoelectric properties of Mn–Al co-doped ZnO ceramics. Journal of the Ceramic Society of Japan, 2016, 124, 515-522.	1.1	22
252	Effects of Processing Parameters on the Deposition of Yttria Partially Stabilized Zirconia Coating During Suspension Plasma Spray. Journal of the American Ceramic Society, 2016, 99, 3546-3555.	3.8	22

Υοςηίο δάκκα

#	Article	IF	CITATIONS
253	Densification kinetics during isothermal sintering of 8YSZ. Journal of the European Ceramic Society, 2016, 36, 1269-1275.	5.7	22
254	Highâ€ŧemperature strength and plastic deformation behavior of niobium diboride consolidated by spark plasma sintering. Journal of the American Ceramic Society, 2017, 100, 5295-5305.	3.8	22
255	Stabilization of Yttria Aqueous Suspension with Polyethylenimine and Electrophoretic Deposition Journal of the Ceramic Society of Japan, 2002, 110, 840-843.	1.3	21
256	Nano-Blast Synthesis of Nano-size CeO2-Gd2O3 Powders. Journal of the American Ceramic Society, 2006, 89, 1822-1826.	3.8	21
257	Effect of Milling Treatment on Texture Development of Hydroxyapatite Ceramics by Slip Casting in High Magnetic Field. Materials Transactions, 2007, 48, 2861-2866.	1.2	21
258	Appearance of high-temperature phase in zirconia films made by aerosol gas deposition method. Journal of the Ceramic Society of Japan, 2011, 119, 271-276.	1.1	21
259	Intensity of sulfonitric treatment on multiwall carbon nanotubes. Chemical Physics Letters, 2017, 689, 135-141.	2.6	21
260	Influence of Washing on Zirconia Powder for Electrophoretic Deposition. Journal of the American Ceramic Society, 2001, 84, 666-668.	3.8	20
261	Microstructural Design for High-Strain-Rate Superplastic Oxide Ceramics. Journal of the Ceramic Society of Japan, 2005, 113, 191-197.	1.3	20
262	Sonochemical Preparation and Properties of Pt-3Y-TZP Nano-Composites. Journal of the American Ceramic Society, 2005, 88, 639-644.	3.8	20
263	Highly controlled orientation of CaBi4Ti4O15 using a strong magnetic field. Applied Physics Letters, 2006, 89, 132902.	3.3	20
264	Fabrication of Textured α-SiC Using Colloidal Processing and a Strong Magnetic Field. Materials Transactions, 2007, 48, 2883-2887.	1.2	20
265	Phosphate Esters as Dispersants for the Cathodic Electrophoretic Deposition of Alumina Suspensions. Journal of the American Ceramic Society, 2008, 91, 1923-1926.	3.8	20
266	Fabrication of GDC/LSGM/GDC tri-layers on polypyrrole-coated NiO-YSZ by electrophoretic deposition for anode-supported SOFC. Journal of the Ceramic Society of Japan, 2009, 117, 1246-1248.	1.1	20
267	Emission color tuning of laminated and mixed SiAlON phosphor films by electrophoretic deposition. Journal of the Ceramic Society of Japan, 2010, 118, 1-4.	1.1	20
268	Effect of Gd2O3 on the thermal conductivity of ZrO2–4mol.% Y2O3 ceramics fabricated by spark plasma sintering. Scripta Materialia, 2013, 69, 165-170.	5.2	20
269	Ideal design of textured LiCoO2 sintered electrode for Li-ion secondary battery. APL Materials, 2013, 1, .	5.1	20
270	Fabrication, microstructure and properties of in situ synthesized B4C^ ^ndash;NbB2 eutectic composites by spark plasma sintering. Journal of the Ceramic Society of Japan, 2015, 123, 33-37.	1.1	20

#	Article	IF	CITATIONS
271	Highly anisotropic single crystal-like La2Ti2O7 ceramic produced by combined magnetic field alignment and templated grain growth. Journal of the European Ceramic Society, 2015, 35, 1771-1776.	5.7	20
272	Columnar and DVC-structured thermal barrier coatings deposited by suspension plasma spray: high-temperature stability and their corrosion resistance to the molten salt. Ceramics International, 2016, 42, 16822-16832.	4.8	20
273	Electrophoretic Deposition of Alumina on Conductive Polymer-Coated Ceramic Substrates. Journal of the Ceramic Society of Japan, 2006, 114, 55-58.	1.3	19
274	A practical technique for the fabrication of highly ordered macroporous structures of inorganic oxides. Materials Research Bulletin, 2006, 41, 268-273.	5.2	19
275	Fabrication of textured alumina by magnetic alignment via gelcasting based on low-toxic system. Journal of the European Ceramic Society, 2014, 34, 3841-3848.	5.7	19
276	Electrophoretic fabrication of a-b plane oriented La2NiO4 cathode onto electrolyte in strong magnetic field for low-temperature operating solid oxide fuel cell. Journal of the European Ceramic Society, 2016, 36, 4077-4082.	5.7	19
277	Layer Structure of Textured CaBi4Ti4O15Ceramics Fabricated by Slip Casting in High Magnetic Field. Journal of the American Ceramic Society, 2007, 90, 1463-1466.	3.8	18
278	Spherical Mesoporous Silica Particles with Titanium Dioxide Nanoparticles by an Aerosol-assisted Coassembly. Chemistry Letters, 2008, 37, 72-73.	1.3	18
279	Preparation of Highly Oriented Transparent (Sr,Ba)Nb2O6Ceramics and Their Ferroelectric Properties. Japanese Journal of Applied Physics, 2009, 48, 031405.	1.5	18
280	Simultaneous alignment and micropatterning of carbon nanotubes using modulated magnetic field. Science and Technology of Advanced Materials, 2009, 10, 014603.	6.1	18
281	Wet Processing and Lowâ€Temperature Pressureless Sintering of SiC Using a Novel Al ₃ BC ₃ Sintering Additive. Journal of the American Ceramic Society, 2009, 92, 2888-2893.	3.8	18
282	Impact of magnetic field on molecular alignment and electrical conductivity in phthalocyanine nanowires. Journal of Materials Chemistry, 2012, 22, 8629.	6.7	18
283	Photoluminescent properties of new up-conversion phosphors of Yb/Tm co-doped (Gd1â^'xLux)3Al5O12 (x=0.1–0.5) garnet solid solutions. Journal of Alloys and Compounds, 2014, 582, 623-627.	5.5	18
284	Fabrication of textured Ti ₃ SiC ₂ ceramic by slip casting in a strong magnetic field and pressureless sintering. Journal of the Ceramic Society of Japan, 2014, 122, 817-821.	1.1	18
285	Consolidation of B4C-TaB2 eutectic composites by spark plasma sintering. Journal of Asian Ceramic Societies, 2015, 3, 369-372.	2.3	18
286	Synthesis of Highly Photocatalytic TiO ₂ Microflowers Based on Solvothermal Approach Using <l>N,N</l> -Dimethylformamide. Journal of Nanoscience and Nanotechnology, 2015, 15, 4747-4751.	0.9	18
287	Development of an electrochemical impedance analysis program based on the expanded measurement model. Journal of the Ceramic Society of Japan, 2016, 124, 943-949.	1.1	18
288	Synthesis of Aligned Alumina by Slip Casting in a High Magnetic Field and Heat Treatment Funtai Oyobi Fummatsu Yakin/Journal of the Japan Society of Powder and Powder Metallurgy, 2000, 47, 1010-1014.	0.2	17

ΥΟSΗΙΟ SAKKA

#	Article	IF	CITATIONS
28	Synthesis and Sintering of Zirconia Nano-Powder by Non-Isothermal Decomposition from Hydroxide Journal of the Ceramic Society of Japan, 2001, 109, 500-505.	1.3	17
29	Alignment of TiO2 particles by electrophoretic deposition in a high magnetic field. Materials Research Bulletin, 2004, 39, 2155-2161.	5.2	17
29	Fluorescence detection and imaging of amino-functionalized organic monolayer. Thin Solid Films, 2008, 516, 2541-2546.	1.8	17
29	Nanoreactor engineering and SPS densification of multimetal oxide ceramic nanopowders. Journal of the European Ceramic Society, 2008, 28, 919-927.	5.7	17
29	Hydrolysis and Dispersion Properties of Aqueous Y ₂ Si ₂ O ₇ Suspensions. Journal of the American Ceramic Society, 2009, 92, 54-61.	3.8	17
29	Simple preparation of silica and alumina with a hierarchical pore system via the dual-templating method. Science and Technology of Advanced Materials, 2009, 10, 025002.	6.1	17
29	Si ₃ N ₄ –TiN Nanocomposite by Nitration of TiSi ₂ and Consolidation by Hot Pressing and Spark Plasma Sintering. Journal of Nanoscience and Nanotechnology, 2009, 9, 6381-6389.	0.9	17
29	Near-infrared photoluminescence and Raman characterization of bismuth-embedded sodalite nanocrystals. Optics Letters, 2010, 35, 1743.	3.3	17
29	White-light-emitting Liquefiable Silicon Nanocrystals. Chemistry Letters, 2012, 41, 1157-1159.	1.3	17
29	 Porous calcium sulfate ceramics with tunable degradation rate. Journal of Materials Science: Materials in Medicine, 2012, 23, 2437-2443. 	3.6	17
29	Synthesis, characterization, and photoluminescent properties of (La0.95Eu0.05)2O2SO4 red phosphors with layered hydroxyl sulfate as precursor. Journal of Alloys and Compounds, 2014, 603, 28-34.	5.5	17
30	Photoluminescent and cathodoluminescent performances of Tb ³⁺ in Lu ³⁺ -stabilized gadolinium aluminate garnet solid-solutions of [(Gd _{1â[°]x} Lu _x) _{1â[°]y} Tb _y] ₃ Al ₅ RSC Advances, 2015, 5, 59686-59695.	O _{12<td>>.¹⁷</td>}	>. ¹⁷
30	Inversion domain boundaries in Mn and Al dualâ€doped ZnO: Atomic structure and electronic properties. Journal of the American Ceramic Society, 2017, 100, 4252-4262.	3.8	17
30	Photoluminescent and scintillant properties of highly transparent [(Y _{1â€} <i>_x</i> Gd <i>_x</i>) _{0.99} Dy _{0.01}]< (<i>xÂ</i> = 0 and 0.4) ceramics. Journal of the American Ceramic Society, 2019, 102, 4773-4780.	sub>2 <b sub>O <s< td=""><td>sub7>3</td></s<>	sub7>3
30	Cation Interdiffusion in Polycrystalline Cubic C-Type Yttria-Zirconia-Hafnia Solid Solutions. Journal of the American Ceramic Society, 1989, 72, 2121-2125.	3.8	16
30	Liquid Manipulation Lithography to Fabricate a Multifunctional Microarray of Organosilanes on an Oxide Surface under Ambient Conditions. Advanced Functional Materials, 2008, 18, 3049-3055.	14.9	16
30	Exploration of a Standing Mesochannel System with Antimatter/Matter Atomic Probes. Advanced Materials, 2008, 20, 4728-4733.	21.0	16
30	Facile patterning of assembled silica nanoparticles with a closely packed arrangement through guided growth. Journal of Materials Chemistry, 2009, 19, 1964.	6.7	16

#	Article	IF	CITATIONS
307	Coexistence of A―and B‧ite Vacancy Compensation in Laâ€Doped Sr _{1â°'<i>x</i>} Ba <i>_x</i> TiO ₃ . Journal of the American Ceramic Society, 2010, 93, 2903-2908.	3.8	16
308	Sensitized broadband near-infrared luminescence from bismuth-doped silicon-rich silica films. Optics Letters, 2011, 36, 4221.	3.3	16
309	Orientation control of mordenite zeolite in strong magnetic field. Microporous and Mesoporous Materials, 2012, 151, 188-194.	4.4	16
310	Electric field in SPS: geometry and pulsed current effects. Journal of the Ceramic Society of Japan, 2013, 121, 524-526.	1.1	16
311	Microwave Sintering of <scp><scp>Ti</scp></scp> ₃ <scp>Si</scp> (<scp>(<scp>Al</scp></scp>) <scp>Co Ceramic. Journal of the American Ceramic Society, 2014, 97, 2731-2735.</scp>	8> <td>:p16sub>2<</td>	:p 16 sub>2<
312	Preparation of macroporous titania from nanoparticle building blocks and polymer templates. Scripta Materialia, 2003, 49, 735-740.	5.2	15
313	Control of Crystal Orientation of Hydroxyapatite by using a High Magnetic Field. Key Engineering Materials, 2003, 240-242, 513-516.	0.4	15
314	Strain Softening and Hardening during Superplasticâ€Like Flow in a Fineâ€Grained MgAl ₂ O ₄ Spinel Polycrystal. Journal of the American Ceramic Society, 2004, 87, 1102-1109.	3.8	15
315	Dispersion of SiC Suspensions with Cationic Dispersant of Polyethylenimine. Journal of the Ceramic Society of Japan, 2005, 113, 584-587.	1.3	15
316	The Effect of Embedding Conditions on the Thermal Conductivity of .BETASi3N4. Journal of the Ceramic Society of Japan, 2006, 114, 1093-1096.	1.3	15
317	Highly Texturing β-Sialon Via Strong Magnetic Field Alignment. Journal of the American Ceramic Society, 2008, 91, 620-623.	3.8	15
318	Texture development in 3mol% yttria-stabilized tetragonal zirconia. Materials Research Bulletin, 2009, 44, 1802-1805.	5.2	15
319	Orientation Dependence of Semiconductor Properties in Anatase TiO[sub 2] Polycrystalline Aggregates. Journal of the Electrochemical Society, 2010, 157, H65.	2.9	15
320	Superplastic deformation of hydroxyapatite ceramics with B2O3 or Na2O addition fabricated by pulse current pressure sintering. Journal of the European Ceramic Society, 2011, 31, 2641-2648.	5.7	15
321	Nanocrystalline ZrB ₂ powders prepared by mechanical alloying. Journal of Asian Ceramic Societies, 2013, 1, 304-307.	2.3	15
322	Twoâ€Ðimensional Orientation in <scp><scp>Bi</scp></scp> ₄ <scp><scp>Ti</scp>3<scp>O</scp></scp> < Prepared Using Platelet Particles and a Magnetic Field. Journal of the American Ceramic Society, 2013, 96, 1085-1089.	sub>12 <td>subչ 15</td>	subչ 15
323	Sintering and Gas Release of Ag Ultrafine Powders. Nippon Kinzoku Gakkaishi/Journal of the Japan Institute of Metals, 1989, 53, 614-620.	0.4	15
324	Hydrogen sorption-desorption characteristics of mixed and composite Niî—,TiN nanoparticles. Scripta Materialia, 1996, 7, 341-353.	0.5	14

ΥΟSΗΙΟ SAKKA

#	Article	IF	CITATIONS
325	Preparation and Characterization of Fine Shirasuballoons. Journal of the Ceramic Society of Japan, 1996, 104, 963-968.	1.3	14
326	Low-temperature preparation of lithium vanadium oxides by solution processing. Journal of the European Ceramic Society, 2004, 24, 405-408.	5.7	14
327	3-Dimensional Grain Orientation of RE-Ba-Cu-O Superconductors Using a Modulated Oval Magnetic Field. IEEE Transactions on Applied Superconductivity, 2009, 19, 2961-2964.	1.7	14
328	Hybrid processing and anisotropic sintering shrinkage in textured ZnO ceramics. Science and Technology of Advanced Materials, 2010, 11, 065006.	6.1	14
329	Significant third-order optical nonlinearity enhancement of gold nanoparticle incorporated mesoporous silica thin films by magnetic field thermal treatment. Journal of Materials Chemistry, 2010, 20, 8399.	6.7	14
330	Influence of the zirconia transformation on the thermal behavior of zircon–zirconia composites. Journal of Thermal Analysis and Calorimetry, 2012, 110, 695-705.	3.6	14
331	Densification Kinetics of Nanocrystalline Zirconia Powder Using Microwave and Spark Plasma Sintering—A Comparative Study. Journal of Nanoscience and Nanotechnology, 2012, 12, 4577-4582.	0.9	14
332	Synthesis, microstructure and mechanical properties of reactively sintered ZrB 2 –SiC–ZrN composites. Ceramics International, 2013, 39, 7273-7277.	4.8	14
333	Analysis of abnormal grain growth of oriented LiCoO2 prepared by slip casting in a strong magnetic field. Journal of the European Ceramic Society, 2013, 33, 3059-3064.	5.7	14
334	Perfect Highâ€Temperature Plasticity Realized in Multiwalled Carbon Nanotubeâ€Concentrated αâ€ <scp><scp>Al</scp></scp> ₂ <scp><scp>O</scp></scp> ₃ Hybrid. Journal of the American Ceramic Society, 2013, 96, 1904-1908.	3.8	14
335	Mechanically reliable thermoelectric (TE) nanocomposites by dispersing and embedding TE-nanostructures inside a tetragonal ZrO2matrix: the concept and experimental demonstration in graphene oxide–3YSZ system. Science and Technology of Advanced Materials, 2014, 15, 014201.	6.1	14
336	Controlled Photocatalytic Growth of Ag Nanocrystals on Brookite and Rutile and Their SERS Performance. ACS Applied Materials & Interfaces, 2014, 6, 236-243.	8.0	14
337	Controlled Crystallization of Cyanoâ€Bridged Cu–Pt Coordination Polymers with Twoâ€Đimensional Morphology. Chemistry - an Asian Journal, 2014, 9, 1511-1514.	3.3	14
338	Synthesis of <i>Multilayered</i> Starâ€5haped B ₆ O Particles Using the Seedâ€Mediated Growth Method. Journal of the American Ceramic Society, 2015, 98, 3635-3638.	3.8	14
339	Yellow-emitting (Tb 1â^'x Ce x) 3 Al 5 O 12 phosphor powder and ceramic (0≤â‰ 0 .05): Phase evolution, photoluminescence, and the process of energy transfer. Ceramics International, 2017, 43, 8163-8170.	4.8	14
340	Surface Phases of Iron Ultrafine Powders Estimated from Thermal Desorption Measurements and Their Reduction Characteristics. Nippon Kinzoku Gakkaishi/Journal of the Japan Institute of Metals, 1991, 55, 219-226.	0.4	14
341	Hydrogen desorption characteristics of composite Co-TiN nanoparticles. Applied Surface Science, 1996, 100-101, 232-237.	6.1	13
342	Development of Thermoelectric Bi-Based Cobaltites with an Easy Axis of Magnetization Parallel to theC-Axis for Magnetic Alignment. Japanese Journal of Applied Physics, 2005, 44, L1263-L1266.	1.5	13

#	Article	IF	CITATIONS
343	Electrophoretic deposition of Eu2+ doped CaALPHASiAlON phosphor particles for packaging of flat pseudo-white light emitting devices. Journal of the Ceramic Society of Japan, 2008, 116, 740-743.	1.1	13
344	Effect of bead-milling treatment on the dispersion of tetragonal zirconia nanopowder and improvements of two-step sintering. Journal of the Ceramic Society of Japan, 2009, 117, 470-474.	1.1	13
345	Fabrication of c-axis oriented zinc oxide by electrophoretic deposition in a rotating magnetic field. Journal of the European Ceramic Society, 2010, 30, 1171-1175.	5.7	13
346	Role of Modification Agent Coverage in Hydrogen Generation by the Reaction of Al with Water. Journal of the American Ceramic Society, 2010, 93, 2534-2536.	3.8	13
347	Texture development in anatase and rutile prepared by slip casting in a strong magnetic field. Journal of the Ceramic Society of Japan, 2011, 119, 334-337.	1.1	13
348	Phase Relation Studies in the ZrO2-CeO2-La2O3 System at 1500°C. Journal of the American Ceramic Society, 2011, 94, 1911-1919.	3.8	13
349	Fabrication and Characterization of Transparent (Y _{0.98â^'<i>x</i>} Tb _{0.02} Eu _{<i>x</i>}) ₂ O ₃ Ceramics with Colorâ€Tailorable Emission. Journal of the American Ceramic Society, 2015, 98, 3877-3883.	3.8	13
350	Highâ€Temperature Strength of Boron Suboxide Ceramic Consolidated by Spark Plasma Sintering. Journal of the American Ceramic Society, 2016, 99, 2769-2777.	3.8	13
351	High temperature flexural strength in monolithic boron carbide ceramic obtained from two different raw powders by spark plasma sintering. Journal of the Ceramic Society of Japan, 2016, 124, 587-592.	1.1	13
352	Highly Segmented Thermal Barrier Coatings Deposited by Suspension Plasma Spray: Effects of Spray Process on Microstructure. Journal of Thermal Spray Technology, 2016, 25, 1638-1649.	3.1	13
353	Hardness and toughness control of brittle boron suboxide ceramics by consolidation of star-shaped particles by spark plasma sintering. Ceramics International, 2016, 42, 3525-3530.	4.8	13
354	Improved galvanic replacement growth of Ag microstructures on Cu micro-grid for enhanced SERS detection of organic molecules. Materials Science and Engineering C, 2016, 61, 97-104.	7.3	13
355	The Crystal Orientation Taking Account of Gravity Force under High Magnetic Field. ISIJ International, 2005, 45, 997-1000.	1.4	13
356	Colloidal Processing for Fine Particles of Al2O3-15vol% ZrO2 System Funtai Oyobi Fummatsu Yakin/Journal of the Japan Society of Powder and Powder Metallurgy, 1997, 44, 356-361.	0.2	12
357	Fabrication of Ordered Macroporous Structures Based on Hetero-Coagulation Process Using Nanoparticle as Building Blocks. Chemistry Letters, 2003, 32, 276-277.	1.3	12
358	Texture of Alumina by Neutron Diffraction and SEM-EBSD. Materials Science Forum, 2005, 495-497, 1395-1400.	0.3	12
359	Texturing behavior in sintered reaction-bonded silicon nitride via strong magnetic field alignment. Journal of the European Ceramic Society, 2008, 28, 929-934.	5.7	12
360	<i>In situ</i> observation of magnetic orientation process of feeble magnetic materials under high magnetic fields. Science and Technology of Advanced Materials, 2008, 9, 024211.	6.1	12

#	Article	IF	CITATIONS
361	Effects of Initial Punch-Die Clearance in Spark Plasma Sintering Process. Materials Transactions, 2008, 49, 2899-2906.	1.2	12
362	Magnetically induced orientation of mesochannels inside porous anodic alumina membranes under ultra high magnetic field of 30 T: Confirmation by TEM. Journal of the Ceramic Society of Japan, 2008, 116, 1244-1248.	1.1	12
363	Low-temperature formation of Ln silicate oxyapatite (Ln=La and Nd) by the water-based sol–gel method. Solid State Ionics, 2011, 204-205, 91-96.	2.7	12
364	Deflocculation and stabilization of Ti ₃ SiC ₂ ceramic powder in gelcasting process. Journal of the Ceramic Society of Japan, 2015, 123, 1010-1017.	1.1	12
365	Synthesis of iron oxide nanoparticles with different morphologies by precipitation method with and with out chitosan addition. Journal of the Ceramic Society of Japan, 2016, 124, 489-494.	1.1	12
366	Low-temperature spark plasma sintering of alumina by using SiC molding set. Journal of the Ceramic Society of Japan, 2016, 124, 1141-1145.	1.1	12
367	Spark Plasma Sintering of Highly Transparent Hydroxyapatite Ceramics. Funtai Oyobi Fummatsu Yakin/Journal of the Japan Society of Powder and Powder Metallurgy, 2017, 64, 547-551.	0.2	12
368	Preparation of Fine Shirasuballoons from Vitric Volcaniclastic Materials Funtai Oyobi Fummatsu Yakin/Journal of the Japan Society of Powder and Powder Metallurgy, 1995, 42, 1128-1135.	0.2	11
369	Effect of MgAl ₂ O ₄ Spinel Dispersion on High-Strain-Rate Superplasticity in Tetragonal ZrO ₂ Polycrystal. Materials Transactions, 2004, 45, 2073-2077.	1.2	11
370	Effect of Bi(B)O3 perovskite substitution on enhanced tetragonality and ferroelectric transition temperature in Pb(Zr,Ti)O3 ceramics. Materials Chemistry and Physics, 2011, 129, 322-325.	4.0	11
371	Textured Ti ₃ SiC ₂ by gelcasting in a strong magnetic field. Journal of the Ceramic Society of Japan, 2012, 120, 544-547.	1.1	11
372	Fabrication and Analysis of the Oriented <scp><scp>LiCoO</scp></scp> ₂ by Slip Casting in a Strong Magnetic Field. Journal of the American Ceramic Society, 2012, 95, 3428-3433.	3.8	11
373	Fabrication of Dense ZrO2/CNT Composites: Influence of Bead-Milling Treatment. Metallurgical and Materials Transactions A: Physical Metallurgy and Materials Science, 2013, 44, 4374-4381.	2.2	11
374	Phosphor Deposits of β-Sialon:Eu2+ Mixed with SnO2 Nanoparticles Fabricated by the Electrophoretic Deposition (EPD) Process. Materials, 2014, 7, 3623-3633.	2.9	11
375	Beta-sialon phosphor deposits fabricated by electrophoretic deposition (EPD) process in a magnetic field. Ceramics International, 2014, 40, 8369-8375.	4.8	11
376	B ₆ O ceramic by <i>in-situ</i> reactive spark plasma sintering of a B ₂ O ₃ and B powder mixture. Journal of the Ceramic Society of Japan, 2014, 122, 336-340.	1.1	11
377	Electrophoretic deposition for obtaining dense lanthanum silicate oxyapatite (LSO). Ceramics International, 2016, 42, 19283-19288.	4.8	11
378	Enhancement of MgO Evaporation from MgO-Stabilized ZrO2 by Grain-Boundary Diffusion. Journal of the American Ceramic Society, 1986, 69, 111-113.	3.8	10

#	Article	IF	CITATIONS
379	Sintering and Gas Desorption Characteristics of Copper Ultrafine Powders. Materials Transactions, JIM, 1990, 31, 802-809.	0.9	10
380	The manufacturing process of fine Shirasu balloons using a fluidized sand-bed furnace. Advanced Powder Technology, 2000, 11, 503-516.	4.1	10
381	Synthesis and Characterization of Nanosize Ceria-Gadolinia Powders. Journal of the Ceramic Society of Japan, 2005, 113, 101-106.	1.3	10
382	Pulsed-DC Electrophoretic Deposition (EPD) of Aqueous Alumina Suspension for Controlling Bubble Incorporation and Deposit Microstructure. Key Engineering Materials, 0, 412, 39-44.	0.4	10
383	Wavelength-Selectivity in Photochemical Reaction Between 1-Alcohol and Hydrogen-Terminated Silicon. Journal of Nanoscience and Nanotechnology, 2009, 9, 666-669.	0.9	10
384	Influence of uni and bi-modal SiC composition on mechanical properties and microstructure of reaction-bonded SiC ceramics. Journal of the Ceramic Society of Japan, 2010, 118, 1028-1031.	1.1	10
385	Near-infrared photoluminescence from molecular crystals containing tellurium. Journal of Materials Chemistry, 2012, 22, 24792.	6.7	10
386	Theoretical modeling of electrode impedance for an oxygen ion conductor and metallic electrode system based on the interfacial conductivity theory. Solid State Ionics, 2013, 232, 49-57.	2.7	10
387	Grain-boundary sliding model of pore shrinkage in late intermediate sintering stage under hydrostatic pressure. Acta Materialia, 2013, 61, 6661-6669.	7.9	10
388	Chemical Reactivity and Cathode Properties of LaCoO ₃ on Lanthanum Silicate Oxyapatite Electrolyte. Key Engineering Materials, 0, 616, 120-128.	0.4	10
389	EDTA-assisted phase conversion synthesis of (Gd _{0.95} RE _{0.05})PO ₄ nanowires (RE = Eu, Tb) and investigation of photoluminescence. Science and Technology of Advanced Materials, 2017, 18, 447-457.	6.1	10
390	Fabrication and Mechanical Properties of Textured Ti ₃ SiC ₂ Systems Using Commercial Powder. Materials Transactions, 2018, 59, 829-834.	1.2	10
391	Sintering characteristics of cobalt ultrafine powders. Journal of the Less Common Metals, 1991, 168, 277-287.	0.8	9
392	Control of Texture in Electroceramics by Slip-Casting in a High Magnetic Field. Key Engineering Materials, 2003, 248, 191-194.	0.4	9
393	Micro-Scale Patterning of Ceramic Colloidal Suspension by Micro Molding in Capillaries (MIMIC) with Assistance of Highly Infiltrating Liquid. Journal of the Ceramic Society of Japan, 2006, 114, 725-728.	1.3	9
394	An efficient matrix that resists the nonspecific adsorption of protein to fabricate carbohydrate arrays on silicon. Thin Solid Films, 2006, 499, 213-218.	1.8	9
395	Effect of grain size on electrical properties of scandia-stabilized zirconia. Journal of the Ceramic Society of Japan, 2010, 118, 1038-1043.	1.1	9
396	Determination of Easy Magnetization Axis of Mordenite Zeolite. Chemistry Letters, 2010, 39, 347-349.	1.3	9

Υοςηίο δάκκα

#	Article	IF	CITATIONS
397	Microstructure Control of Barium Titanate – Potassium Niobate Solid Solution System Ceramics by MPB Engineering and their Piezoelectric Properties. Key Engineering Materials, 2011, 485, 89-92.	0.4	9
398	Fabrication of the c-axis oriented zeolite L compacts using strong magnetic field. Materials Letters, 2013, 93, 408-410.	2.6	9
399	Challenges of nanostructuring and functional properties for selected bulk materials obtained by reactive spark plasma sintering. Japanese Journal of Applied Physics, 2014, 53, 05FB22.	1.5	9
400	Consolidation of B ₄ C–VB ₂ eutectic ceramics by spark plasma sintering. Journal of the Ceramic Society of Japan, 2015, 123, 1051-1054.	1.1	9
401	Inversion domain network stabilization and spinel phase suppression in ZnO. Journal of the American Ceramic Society, 2018, 101, 2616-2626.	3.8	9
402	Preparation and Properties of Lightweight Pottery Using Shirasuballoon. Journal of the Ceramic Society of Japan, 1998, 106, 333-338.	1.3	8
403	Cavity Damage Accumulation in Alumina Doped with Zirconia or Magnesia. Materials Science Forum, 1999, 304-306, 431-436.	0.3	8
404	Effect of cavitation on superplastic flow of 10% zirconia-dispersed alumina. Scripta Materialia, 2001, 45, 61-67.	5.2	8
405	Area-selective assembly of high crystalline tin-doped–indium–oxide particles onto monolayer template. Journal of Vacuum Science and Technology A: Vacuum, Surfaces and Films, 2005, 23, 1146-1151.	2.1	8
406	Nano-explosion synthesis of multi-component ceramic nano-composites. Journal of the European Ceramic Society, 2007, 27, 585-592.	5.7	8
407	Photoanode characteristics of dye-sensitized solar cell containing TiO2 layers with different crystalline orientations. Journal of Materials Research, 2009, 24, 1417-1421.	2.6	8
408	Dispersion and Shortening of Multi-Walled Carbon Nanotubes by Size Modification. Materials Transactions, 2010, 51, 192-195.	1.2	8
409	Magnetic field-induced off-resonance third-order optical nonlinearity of iron oxide nanoparticles incorporated mesoporous silica thin films during heat treatment. Optics Express, 2010, 18, 2010.	3.4	8
410	Textured lead titanate ceramics fabricated by slip casting under a high magnetic field. Journal of the Ceramic Society of Japan, 2011, 119, 60-64.	1.1	8
411	Fabrication of the oriented LiCoO2 sheet using a strong magnetic field. Journal of the Ceramic Society of Japan, 2011, 119, 701-705.	1.1	8
412	One-step route to a hybrid TiO2/TixW1â^'xN nanocomposite byin situselective carbothermal nitridation. Science and Technology of Advanced Materials, 2012, 13, 035001.	6.1	8
413	Effective preparation of SiC nanoparticles by the reaction of thermal nitrogen plasma with solid SiC. Journal of Alloys and Compounds, 2012, 520, 127-131.	5.5	8
414	Mechanochemical activation of aluminum powder and synthesis of alumina based ceramic composites. Ceramics International, 2013, 39, 8141-8146.	4.8	8

#	Article	IF	CITATIONS
415	Theoretical modeling of electrode impedance for an oxygen ion conductor and metallic electrode system based on the interfacial conductivity theory. Part II: Case of the limiting process by non-steady-state surface diffusion. Solid State Ionics, 2013, 249-250, 78-85.	2.7	8
416	Discovery of a new crystalline phase: BiGeO ₂ (OH) ₂ (NO ₃). CrystEngComm, 2014, 16, 10080-10088.	2.6	8
417	Positional-dependent luminescence property of β-SiAlON:Eu2+ phosphor particle. Applied Physics Letters, 2014, 104, .	3.3	8
418	Microstructure and adsorption property of nanocarbide-derived carbon (CDC) synthesized at ambient temperature. Materials Letters, 2014, 130, 188-191.	2.6	8
419	Sinterable powder fabrication of lanthanum silicate oxyapatite based on solid-state reaction method. Journal of the Ceramic Society of Japan, 2015, 123, 274-279.	1.1	8
420	Fabrication of (111)-oriented Tetragonal BaTiO ₃ Ceramics by an Electrophoretic Deposition in a High Magnetic Field. Transactions of the Materials Research Society of Japan, 2015, 40, 223-226.	0.2	8
421	Processing and enhanced piezoelectric properties of highly oriented compositionally modified Pb(Zr,Ti)O ₃ ceramics fabricated by magnetic alignment. Applied Physics Express, 2015, 8, 041501.	2.4	8
422	Properties of Fine Shirasuballoons. Journal of the Ceramic Society of Japan, 1997, 105, 79-84.	1.3	7
423	Fracture Toughness of Yttria-Stabilized Cubic Zirconia (8Y-CSZ) Doped with Pure Silica. Materials Transactions, 2004, 45, 3324-3329.	1.2	7
424	One-Dimensional Self-Assembly of Alkoxy-Capped Silicon Nanoparticles. Journal of Nanoscience and Nanotechnology, 2006, 6, 1823-1825.	0.9	7
425	Large-Scale Patterning of TiO2 Nano Powders Using Micro Molds. Journal of the Ceramic Society of Japan, 2007, 115, 697-700.	1.1	7
426	Improvement of thermoelectric performance in magnetically c-axis-oriented bismuth-based cobaltites. Scripta Materialia, 2007, 57, 333-336.	5.2	7
427	Control of lattice spacing in a triangular lattice of feeble magnetic particles formed by induced magnetic dipole interactions. Science and Technology of Advanced Materials, 2009, 10, 014608.	6.1	7
428	Aqueous Dispersions of Carbon Nanotubes Stabilized by Zirconium Acetate. Journal of Nanoscience and Nanotechnology, 2009, 9, 662-665.	0.9	7
429	Synthesis of SiC nano-powders from liquid carbon and various silica sources. Journal of the Ceramic Society of Japan, 2010, 118, 345-348.	1.1	7
430	Controlled organic/inorganic interface leading to the size-tunable luminescence from Si nanoparticles. Journal of the Ceramic Society of Japan, 2010, 118, 932-939.	1.1	7
431	Influence of La2O3 addition on thermophysical properties of ZrO2-4 mol %Y2O3 ceramics fabricated by spark plasma sintering. Journal of the Ceramic Society of Japan, 2011, 119, 929-932.	1.1	7
432	Phase relationships in the quasi-ternary LaO1.5–SiO2–MgO system at 1773 K. Science and Technology of Advanced Materials, 2012, 13, 045006.	6.1	7

#	Article	IF	CITATIONS
433	Optical and adhesive properties of composite silica-impregnated Ca-α-SiAlON:Eu2+ phosphor films prepared on silica glass substrates. Journal of the European Ceramic Society, 2012, 32, 1365-1369.	5.7	7
434	Damage and wear resistance of Al ₂ O ₃ –CNT nanocomposites fabricated by spark plasma sintering. Journal of the Ceramic Society of Japan, 2013, 121, 867-872.	1.1	7
435	Fabrication of textured \hat{l}_{\pm} -alumina in high magnetic field via gelcasting with the use of glucose derivative. Journal of the Ceramic Society of Japan, 2013, 121, 89-94.	1.1	7
436	Preparation of siloxane-containing vaterite doped with magnesium. Journal of the Ceramic Society of Japan, 2014, 122, 1010-1015.	1.1	7
437	Room-temperature synthesis of Bi ₄ Ge ₃ O ₁₂ from aqueous solution. Japanese Journal of Applied Physics, 2015, 54, 06FJ03.	1.5	7
438	Triaxial Crystalline Orientation of MgTi ₂ O ₅ Achieved Using a Strong Magnetic Field and Geometric Effect. Journal of the American Ceramic Society, 2016, 99, 1852-1854.	3.8	7
439	Photoluminescence efficiency significantly enhanced by surface modification of SiO2 coating on β-sialon:Eu2+ phosphor particle. Journal of Alloys and Compounds, 2018, 741, 454-458.	5.5	7
440	Fabrication of Ceramics with Highly Controlled Microstructures by Advanced Fine Powder Processing. KONA Powder and Particle Journal, 2019, 36, 114-128.	1.7	7
441	Pulsed electrodischarged pressure sintering and flash sintering, a review. Materials Today: Proceedings, 2019, 16, 14-24.	1.8	7
442	Elastic isotropy originating from heterogeneous interlayer elastic deformation in a Ti3SiC2 MAX phase with a nanolayered crystal structure. Journal of the European Ceramic Society, 2021, 41, 2278-2289.	5.7	7
443	Mechanical and magnetic properties of the rapidly quenched Cu2MnAl. Journal of Materials Science, 1990, 25, 2549-2556.	3.7	6
444	Sorption and Desorption Characteristics of Water Vapour on YBa2Cu3O7-xPowders. Japanese Journal of Applied Physics, 1990, 29, L2022-L2025.	1.5	6
445	Sintering and Ionic Conductivity of CuO-Doped Tetragonal ZrO2 Prepared by Novel Colloidal Processing Journal of the Ceramic Society of Japan, 2001, 109, 1004-1009.	1.3	6
446	Electrical Conductivity of a 3Y-TZP/Alumina Laminate Composite Synthesized by Electrophoretic Deposition Journal of the Ceramic Society of Japan, 2002, 110, 959-962.	1.3	6
447	High-Strain-Rate Superplasticity in 3mol%-Y ₂ 0 ₃ -Stabilized Tetragonal ZrO ₂ Dispersed with 30vol% MgAl ₂ 0 ₄ Spinel. Materials Science Forum, 2004, 447-448, 329-334	0.3	6
448	Colloidal Processing and Ionic Conductivity of Fineâ€Grained Cupricâ€Oxideâ€Doped Tetragonal Zirconia. Journal of the American Ceramic Society, 2001, 84, 2129-2131.	3.8	6
449	Bone-like Layer Growth and Adhesion of Osteoblast-like Cells on Calcium-deficient Hydroxyapatite Synthesized at Different pH. Materials Transactions, 2004, 45, 1782-1787.	1.2	6
450	Preparation and proton conductivity of monodisperse nanocrystals of pyrochlore-type antimonic acid and its niobium-substituted materials. Electrochimica Acta, 2005, 50, 3205-3209.	5.2	6

#	Article	IF	CITATIONS
451	Surface design of monolayer-template for reproducible microfabrication of metal oxide film. Thin Solid Films, 2006, 499, 293-298.	1.8	6
452	Texturing CaALPHASialon Via Strong Magnetic Field Alignment. Journal of the Ceramic Society of Japan, 2007, 115, 701-705.	1.1	6
453	Texturing of Si ₃ N ₄ Ceramics via Strong Magnetic Field Alignment. Key Engineering Materials, 2008, 368-372, 871-874.	0.4	6
454	Material properties controlling photocurrent on TiO2 aggregates with plane orientation for dye-sensitized solar cells. Journal of Nanoparticle Research, 2010, 12, 2621-2628.	1.9	6
455	Hybrid dandelion-like YH(O3PC6H5)2:Ln (Ln = Eu3+, Tb3+) particles: formation mechanism, thermal and photoluminescence properties. CrystEngComm, 2011, 13, 5226.	2.6	6
456	3rd International Congress on Ceramics (ICC3). IOP Conference Series: Materials Science and Engineering, 2011, 18, 001001.	0.6	6
457	Alignment of Carbon Nanofibers in the Al ₂ O ₃ Matrix under a Magnetic Field. Materials Transactions, 2011, 52, 572-575.	1.2	6
458	Fabrication of Textured Ti2AlN Ceramic by Slip Casting in a Strong Magnetic Field and Spark Plasma Sintering. Funtai Oyobi Fummatsu Yakin/Journal of the Japan Society of Powder and Powder Metallurgy, 2014, 61, 538-543.	0.2	6
459	Systematic study on densification of alumina fine powder during milliwave sintering at 28ÂGHz. Journal of Asian Ceramic Societies, 2014, 2, 215-222.	2.3	6
460	Nano ZrO ₂ –TiN composites with high strength and conductivity. Journal of the Ceramic Society of Japan, 2015, 123, 86-89.	1.1	6
461	Research and Development of the Coprecipitation Process for Lanthanum Germanate Oxyapatite. Journal of the American Ceramic Society, 2015, 98, 66-70.	3.8	6
462	Microstructural analysis and thermoelectric properties of Sn-Al co-doped ZnO ceramics. AIP Conference Proceedings, 2016, , .	0.4	6
463	Magnetic field alignment in highly concentrated suspensions for gelcasting process. Ceramics International, 2016, 42, 294-301.	4.8	6
464	Preparation of carbamate-containing vaterite particles for strontium removal in wastewater treatment. Journal of Asian Ceramic Societies, 2017, 5, 364-369.	2.3	6
465	Influence of the porosity caused by incomplete sintering on the mechanical behaviour of lanthanum silicate oxyapatite. Ceramics International, 2018, 44, 14348-14354.	4.8	6
466	Gas Evolution and Densification during Sintering of Ultrafine Copper Powders. Nippon Kinzoku Gakkaishi/Journal of the Japan Institute of Metals, 1989, 53, 422-428.	0.4	5
467	Reduction and sintering of ultrafine copper powders. Journal of Materials Science Letters, 1989, 8, 273-276.	0.5	5
468	Effects of cold isostatic pressures on the sintering behaviour of iron and copper ultrafine powders. Journal of Materials Science Letters, 1991, 10, 426-428.	0.5	5

#	Article	IF	CITATIONS
469	Zirconium-Hafnium Interdiffusion in Polycrystalline Fluorite-Cubic CeO2ZrO2HfO2 Solid Solution. Journal of the American Ceramic Society, 1993, 76, 1381-1383.	3.8	5
470	Microstructural examination in high-strain-rate superplastically deformed tetragonal ZrO2 dispersed with 30 vol% MgAl2O4 spinel. Journal of Materials Research, 2007, 22, 801-813.	2.6	5
471	New Processing of Textured Ceramics by Colloidal Processing Under High Magnetic Field. Key Engineering Materials, 2005, 280-283, 721-728.	0.4	5
472	Micro gas sensor assembly of tin oxide nano-particles by a capillary micro-molding process. Journal of the Ceramic Society of Japan, 2010, 118, 202-205.	1.1	5
473	Formation of Zirconia Films by the Aerosol Gas Deposition Method (By Jetting of Positive Charged) Tj ETQq1 1 0 2011, 58, 463-472.	.784314 r 0.2	gBT /Overloc 5
474	Tough Yttria-Stabilized Zirconia Ceramic by Low-Temperature Spark Plasma Sintering of Long-Term Stored Nanopowders. Journal of Nanoscience and Nanotechnology, 2011, 11, 7901-7909.	0.9	5
475	Electrical conductivity and X-ray diffraction analysis of oxyapatite-type lanthanum silicate and neodymium silicate solid solution. Solid State Ionics, 2012, 225, 443-447.	2.7	5
476	Spark Plasma Sintered Ni-YSZ/YSZ Bi-Layers for Solid Oxide Fuel Cell. Journal of Nanoscience and Nanotechnology, 2013, 13, 4150-4157.	0.9	5
477	Electrophoretic deposition of orientation-controlled zeolite L layer on porous ceramic substrate. Journal of the Ceramic Society of Japan, 2013, 121, 370-372.	1.1	5
478	Reductant-Free Colloidal Synthesis of Near-IR Emitting Germanium Nanocrystals: Role of Primary Amine. Journal of Nanoscience and Nanotechnology, 2014, 14, 2204-2210.	0.9	5
479	Significantly improved photoluminescence of the greenâ€emitting βâ€sialon:Eu ²⁺ phosphor via surface coating of TiO ₂ . Journal of the American Ceramic Society, 2019, 102, 294-302.	3.8	5
480	Effects of cold isostatic pressure on the sintering behaviour of nickel ultrafine powders. Journal of Alloys and Compounds, 1992, 190, 31-33.	5.5	4
481	Pressure Filtration of Al2O3 Small Powder Funtai Oyobi Fummatsu Yakin/Journal of the Japan Society of Powder and Powder Metallurgy, 1995, 42, 309-313.	0.2	4
482	Preparation of Polycrystalline Antimonic Acid Films by Electrophoretic Deposition. Journal of Sol-Gel Science and Technology, 2000, 19, 595-598.	2.4	4
483	Preparation and lithium insertion property of layered LixV2O5·nH2O. Journal of Power Sources, 2003, 119-121, 201-204.	7.8	4
484	Porous Al2O3/Al catalyst supports fabricated by an Al(OH)3/Al mixture and the effect of agglomerates. Journal of Materials Research, 2005, 20, 672-679.	2.6	4
485	High Strain-Rate Superplastic Flow in ZrO ₂ -30vol% Spinel Composite. Materials Science Forum, 2005, 475-479, 2977-2980.	0.3	4
486	<i>In Situ</i> Microscopic Observations of Magnetic Field Effects on the Growth of Silver Dendrites. Materials Transactions, 2007, 48, 2888-2892.	1.2	4

#	Article	IF	CITATIONS
487	Zirconia Nanoceramic via Redispersion of Highly Agglomerated Nanopowder and Spark Plasma Sintering. Journal of Nanoscience and Nanotechnology, 2010, 10, 6634-6640.	0.9	4
488	Photoelectrochemical evaluation of anatase TiO ₂ polycrystalline aggregation layers with different crystalline orientations. Journal of Materials Research, 2010, 25, 63-68.	2.6	4
489	Texture development of surface-modified SiC prepared by EPD in a strong magnetic field. Journal of the Ceramic Society of Japan, 2011, 119, 667-671.	1.1	4
490	Preparation and Characterization of Grain-Oriented Barium Titanate Ceramics Using Electrophoresis Deposition Method under a High Magnetic Field. Key Engineering Materials, 2011, 485, 313-316.	0.4	4
491	High-temperature phase in zirconia film fabricated by aerosol gas deposition and its change upon subsequent heat treatment. Journal of the Ceramic Society of Japan, 2013, 121, 333-337.	1.1	4
492	Luminescence Behaviors of the New Upconversion Phosphors of Yb/Ho Co-Doped (Gd _{1-<i>x</i>} Lu _{<i>x</i>}) _{3(x=0.1-0.5) Garnet Solid Solutions. Key Engineering Materials, 0, 602-603, 1034-1038.}	b>4Al&l	t;s 4 b>5<
493	Magnesium ion distribution and defect concentrations of MgO-doped lanthanum silicate oxyapatite. Solid State Ionics, 2014, 258, 24-29.	2.7	4
494	Dispersion and structural evolution of multi-walled carbon nanotubes in ZrB2 matrix. Ceramics International, 2017, 43, 10533-10539.	4.8	4
495	Interphase coordination design in carbamate-siloxane/vaterite composite microparticles towards tuning ion-releasing properties. Advanced Powder Technology, 2017, 28, 1349-1355.	4.1	4
496	Heterocoagulation and SPS sintering of sulfonitric-treated CNT and 8YZ nanopowders. Journal of Asian Ceramic Societies, 2019, 7, 238-246.	2.3	4
497	Fabrication of Textured BaTiO ₃ Ceramics by Electrophoretic Deposition in A High Magnetic Field using Single-domain Particles. Transactions of the Materials Research Society of Japan, 2013, 38, 41-44.	0.2	4
498	Green synthesis, structure feature and energy transfer of yellowâ€emitting (Y,Gd) ₂ O ₂ SO ₄ :Dy phosphors. Luminescence, 2022, 37, 199-207.	2.9	4
499	Permanent deformation of (Co, Ni)Zr intermetallic compounds through phase transformation. Journal of Materials Science, 1989, 24, 2891-2897.	3.7	3
500	Characterization of the Surface Oxide Layer of Iron Ultrafine Particles Nippon Kagaku Kaishi / Chemical Society of Japan - Chemistry and Industrial Chemistry Journal, 1993, 1993, 92-97.	0.1	3
501	Superplastic Tensile Ductility in a Zirconia-Dispersed Alumina Produced by Colloidal Processing. Materials Science Forum, 1999, 304-306, 489-494.	0.3	3
502	High Temperature Deformation of a Yttria-Stabilized Tetragonal Zirconia. Materials Science Forum, 2001, 357-359, 187-192.	0.3	3
503	Fabrication of Textured Alumina through Slip Casting in a High Magnetic Field and Heating. Key Engineering Materials, 2001, 206-213, 349-352.	0.4	3
504	Fabrication of Tailored Alumina-Based Ceramics Through Colloidal Processing. Key Engineering Materials, 2002, 224-226, 619-622.	0.4	3

#	Article	IF	CITATIONS
505	Assembly of hydrothermally synthesized tin oxide nanocrystals. Journal of Vacuum Science and Technology A: Vacuum, Surfaces and Films, 2005, 23, 731-736.	2.1	3
506	Multiple Nano-Blast Synthesis of PT/8Y-ZP Composite Nanopowders. Journal of Nanoscience and Nanotechnology, 2006, 6, 1625-1631.	0.9	3
507	Aqueous Processing of Textured Silicon Nitride Ceramics by Slip Casting in a Strong Magnetic Field. Materials Science Forum, 2007, 534-536, 1009-1012.	0.3	3
508	Fabrication and Some Properties of Textured Ceramics by Colloidal Processing in High Magnetic Field. Key Engineering Materials, 2007, 352, 101-106.	0.4	3
509	Synthesis of Titania Thin Films by Cathodic Electrolytic Deposition. Journal of the Ceramic Society of Japan, 2007, 115, 818-820.	1.1	3
510	Fabrication of Ceria- and Lanthanium Gallate-based Solid Electrolyte Layers on Porous NiO-YSZ by Sequential Electrophoretic Deposition Process. Funtai Oyobi Fummatsu Yakin/Journal of the Japan Society of Powder and Powder Metallurgy, 2012, 59, 626-630.	0.2	3
511	Spark plasma sintering of damage tolerant and machinable YAM ceramics. Journal of Advanced Ceramics, 2013, 2, 193-200.	17.4	3
512	Low-Tepmerature Synthesis Process of Lanthanum Germanate Oxyapatite by Citrate Combustion Method. Funtai Oyobi Fummatsu Yakin/Journal of the Japan Society of Powder and Powder Metallurgy, 2014, 61, 582-586.	0.2	3
513	Metal-Ceramic/Ceramic Nanostructured Layered Composites for Solid Oxide Fuel Cells by Spark Plasma Sintering. Journal of Nanoscience and Nanotechnology, 2014, 14, 4218-4223.	0.9	3
514	Influence of the crystal structure on the physical properties of monoclinic ZrO 2 nanocrystals. Nano Structures Nano Objects, 2015, 1, 1-6.	3.5	3
515	Stabilization of the high-temperature phase and total conductivity of yttrium-doped lanthanum germanate oxyapatite. Journal of the Ceramic Society of Japan, 2018, 126, 91-98.	1.1	3
516	Comparative Investigation on Upconversion Luminescence Properties of Lu 2 O 3 :Er/Yb and Lu 2 O 2 S:Er/Yb Phosphors. Physica Status Solidi (A) Applications and Materials Science, 2021, 218, 2100014.	1.8	3
517	Production of crystal-oriented lanthanum silicate oxyapatite ceramics with anisotropic electrical conductivity and thermal expansion. Open Ceramics, 2021, 6, 100100.	2.0	3
518	Fabrication of Textured Porous Ti ₃ SiC ₂ by Slip Casting under High Magnetic Field and Microstructural Evolution through High Temperature Deformation. Nippon Kinzoku Gakkaishi/Journal of the Japan Institute of Metals, 2021, 85, 256-263.	0.4	3
519	'Beautiful' unconventional synthesis and processing technologies of superconductors and some other materials. Science and Technology of Advanced Materials, 2011, 12, 013001.	6.1	3
520	Fabrication of Textured Porous Ti ₃ SiC ₂ by Slip Casting under High Magnetic Field and Microstructural Evolution through High Temperature Deformation. Materials Transactions, 2022, 63, 133-140.	1.2	3
521	Gas adsorption and desorption characteristics of oxide superconducting powders Funtai Oyobi Fummatsu Yakin/Journal of the Japan Society of Powder and Powder Metallurgy, 1990, 37, 761-764.	0.2	2
522	Control of Texture in Al ₂ 0 ₃ Composites by Slip Casting in a Strong Magnetic Field Followed by Heating. Key Engineering Materials, 2004, 264-268, 245-248.	0.4	2

#	Article	IF	CITATIONS
523	Direct Shaping of Alumina Ceramics by Electrophoretic Deposition Using Conductive Polymer-Coated Ceramic Substrates. Advanced Materials Research, 2007, 29-30, 227-230.	0.3	2
524	Preparation and Utilization of Fine Expanded Perlite. Key Engineering Materials, 0, 280-283, 701-706.	0.4	2
525	Nano Ceramics Center, National Institute for Materials Science. Science and Technology of Advanced Materials, 2007, 8, 571-577.	6.1	2
526	Electrical conductivity of Gd-doped ceria with nano-sized grain. Transactions of the Materials Research Society of Japan, 2009, 34, 555-559.	0.2	2
527	Formation of Crystalline-Oriented Titania Thin Films on ITO Glass Electrodes by EPD in a Strong Magnetic Field. Key Engineering Materials, 2009, 412, 143-148.	0.4	2
528	Electrophretic Deposition of LDC/LSGM/LDC Tri-layers on NiO-YSZ for Anode-supported SOFC. Transactions of the Materials Research Society of Japan, 2010, 35, 723-725.	0.2	2
529	Fabrication of Highly-Densified Hydroxyapatite Ceramic with Boron Oxide Addition and Its Superplastic Deformation. IOP Conference Series: Materials Science and Engineering, 2011, 18, 022020.	0.6	2
530	Application of new low toxic monomers in gelcasting process of alumina powder. IOP Conference Series: Materials Science and Engineering, 2011, 18, 072009.	0.6	2
531	Preparation and Dielectric Properties of Dense Barium Titanate Nanoparticle Accumulations by Electrophoresis Deposition Method. Key Engineering Materials, 2011, 485, 35-38.	0.4	2
532	Textured Ti ₃ SiC ₂ by EPD in a Strong Magnetic Field. Key Engineering Materials, 0, 507, 15-19.	0.4	2
533	Development of High-Strain-Rate Superplastic Oxide Ceramics Based on Flow Mechanism. Materials Science Forum, 2012, 735, 9-14.	0.3	2
534	Preparation of Barium Titanate Grain-Oriented Ceramics by Electrophoresis Deposition Method under High Magnetic Field Using Single-Domain Nanoparticles. Key Engineering Materials, 2013, 582, 27-31.	0.4	2
535	Crystalline-Oriented Beta-Sialon:Eu2+Deposits Fabricated by Electrophoretic Deposition (EPD) within Strong Magnetic Field. ECS Journal of Solid State Science and Technology, 2014, 3, R195-R199.	1.8	2
536	Fabrication of Textured Ti3SiC2 Ceramics by Slip Casting in a Magnetic Field and Pulsed Electric Current Sintering. Journal of the Society of Powder Technology, Japan, 2014, 51, 163-168.	0.1	2
537	Effects of high magnetic fields on thermal convection of conductive aqueous solution. Japanese Journal of Applied Physics, 2015, 54, 077301.	1.5	2
538	Synthesis of crystallographically oriented olivine aggregates using colloidal processing in a strong magnetic field. Physics and Chemistry of Minerals, 2016, 43, 689-706.	0.8	2
539	Fabrication and Mechanical Properties of Textured Ti ₃ SiC ₂ MAX Phase Systems. Funtai Oyobi Fummatsu Yakin/Journal of the Japan Society of Powder and Powder Metallurgy, 2016, 63, 970-975.	0.2	2
540	Dispersion and Reinforcing Mechanism of Carbon Nanotubes in a Ceramic Material. Funtai Oyobi Fummatsu Yakin/Journal of the Japan Society of Powder and Powder Metallurgy, 2016, 63, 955-964.	0.2	2

#	Article	IF	CITATIONS
541	Sedimentation classification treatment effect of starting powders in slip casting on magneto-orientation of mordenite zeolite. Transactions of the Materials Research Society of Japan, 2010, 35, 701-703.	0.2	2
542	Gas evolution characteristics of palladium ultrafine powders Funtai Oyobi Fummatsu Yakin/Journal of the Japan Society of Powder and Powder Metallurgy, 1990, 37, 508-512.	0.2	1
543	Electro-discharge Sintering of (Fe,Co)-B and Ni-B Amorphous Ultrafine Powders Prepared by Chemical Reduction Funtai Oyobi Fummatsu Yakin/Journal of the Japan Society of Powder and Powder Metallurgy, 1995, 42, 323-329.	0.2	1
544	Synthesis of LiSbO3 from Metal Alkoxides Funtai Oyobi Fummatsu Yakin/Journal of the Japan Society of Powder and Powder Metallurgy, 1995, 42, 603-607.	0.2	1
545	Preparation, Electrical Properties, and Water Adsorption Behavior of (1-x)Sb2O5·xM2O3·nH2O (M = Al,) Tj ET	[Qq]] 0.7	'84314 rgBT
546	Microstructure and Superplasticity in Various Zirconia-Dispersed Aluminas Journal of the Ceramic Society of Japan, 2002, 110, 927-930.	1.3	1
547	High-Toughness Tetragonal Zirconia and Zirconia/Alumina Nano-Ceramics. Key Engineering Materials, 2004, 264-268, 2347-2350.	0.4	1
548	Fabrication of Grain-Aligned Bulks and Thick Films of Misfit Layered Cobalt Oxides by a Magneto-Scientific Process. Materials Research Society Symposia Proceedings, 2005, 886, 1.	0.1	1
549	Microstructural Design for Attaining High-Strain-Rate Superplasticity in Oxide Materials. Advances in Science and Technology, 2006, 45, 923.	0.2	1
550	High-Toughness Tetragonal Zirconia/Alumina Nano-Ceramics. Key Engineering Materials, 2006, 317-318, 615-618.	0.4	1
551	Preparation and Properties of Al ₂ O ₃ -Mullite-SiC Nano-Composite by Slip Casting in a High Magnetic Field and Reaction Sintering. Key Engineering Materials, 2007, 336-338, 1133-1136.	0.4	1
552	Synthesis and Properties of Multimetal Oxide Nanopowders via Nano-Explosive Technique. Materials Science Forum, 2007, 534-536, 125-128.	0.3	1
553	Focus on materials analysis and processing in magnetic fields. Science and Technology of Advanced Materials, 2009, 10, 010301.	6.1	1
554	Control of Residual Stress in Multilayered Alumina Composites Prepared Using EPD in a Strong Magnetic Field. Key Engineering Materials, 0, 412, 233-236.	0.4	1
555	Fabrication of Textured Hematite via Topotactic Transformation of Textured Goethite. Applied Physics Express, 2009, 2, 101601.	2.4	1
556	Synthesis, Microstructure and Mechanical Properties of ZrB ₂ Ceramic Prepared by Mechanical Alloying and Spark Plasma Sintering. Key Engineering Materials, 2010, 434-435, 165-168.	0.4	1
557	Fabrication of dense \hat{l}^2 -calcium orthophosphate with submicrometer-sized grains and its high-temperature superplastic deformation. Journal of Materials Science, 2011, 46, 1956-1962.	3.7	1
558	Orientation Control of Hematite via Transformation of Textured Goethite Prepared by EPD in a Strong Magnetic Field. Key Engineering Materials, 2012, 507, 227-231.	0.4	1

#	Article	IF	CITATIONS
559	Structural Features and Color Tunable Photoluminescence of the Binary and Ternary Layered Rare-Earth Hydroxides of (Y,Ln) ₂ (OH) ₅ NO ₃ · <i>n</i> H< (Ln=Tb, Eu). Key Engineering Materials, 0, 544, 252-258.	;sub>2	
560	Hydrothermal transformation of magnetically orientation-controlled seed layer into orientation-retained dense, continuous film in clear reaction solution. Journal of the Ceramic Society of Japan, 2013, 121, 550-554.	1.1	1
561	<i>In Situ</i> Observation of Diamagnetic Fluid Flow in High Magnetic Fields. Key Engineering Materials, 2014, 616, 188-193.	0.4	1
562	Fabrication of Dense Nanostructured Bulk Ceramics by Means of Spark-Plasma-Sintering (SPS) Processing. Materials Science Forum, 2016, 838-839, 225-230.	0.3	1
563	Controlled Surface for Enhanced Luminescence Quantum Yields of Silicon Nanocrystals. Funtai Oyobi Fummatsu Yakin/Journal of the Japan Society of Powder and Powder Metallurgy, 2019, 66, 145-157.	0.2	1
564	Control of the Texture in Feeble Magnetic Ceramics Using Colloidal Processing in a Strong Magnetic Field. Funtai Oyobi Fummatsu Yakin/Journal of the Japan Society of Powder and Powder Metallurgy, 2006, 53, 479-487.	0.2	1
565	Fabrication of Textured Ceramics Using Mn and Nb-doped Hexagonal BaTiO ₃ by an Electrophoretic Deposition in a High Magnetic Field. Transactions of the Materials Research Society of Japan, 2014, 39, 199-202.	0.2	1
566	Effects of Pretreatment of Source Powder Mixture on Aerosol Gas Deposition Film Synthesis and Luminescence. Funtai Oyobi Fummatsu Yakin/Journal of the Japan Society of Powder and Powder Metallurgy, 2017, 64, 558-562.	0.2	1
567	Orientation Dependence of Plastic Deformation Behavior and Fracture Energy Absorption Mechanism around Vickers Indentation of Textured Ti ₃ SiC ₂ Sintered Body. Funtai Oyobi Fummatsu Yakin/Journal of the Japan Society of Powder and Powder Metallurgy, 2020, 67, 607-614.	0.2	1
568	Synthesis and Characterization of the Mixed and the Composite Ni-TiN Utrafine Particles. , 1989, , 203-212.		0
569	Improvement of the hard magnetic properties in Mn-Al-X (X = C, Ti) systems by twin-roll quenching. Journal of Materials Science Letters, 1989, 8, 1123-1126.	0.5	0
570	Preparation and Some Electrical Properties of Yttrium-Doped Antimonic Acids ChemInform, 2003, 34, no.	0.0	0
571	Role of Deformable Fine Spinel Particles in High-Strain-Rate Superplastic Flow of Tetragonal ZrO2. Materials Research Society Symposia Proceedings, 2004, 821, 288.	0.1	0
572	High-Strain Rate Superplastic Zirconia Systems. Key Engineering Materials, 2004, 264-268, 285-288.	0.4	0
573	CONTROL OF PARTICLE ORIENTATION OF HYDROXYAPATITE UNDER A HIGH MAGNETIC FIELD. Phosphorus Research Bulletin, 2005, 19, 256-261.	0.6	0
574	Fracture Toughness of Yttria-Stabilized Cubic Zirconia (8Y-CSZ) Doped with Pure Silica. Nippon Kinzoku Gakkaishi/Journal of the Japan Institute of Metals, 2005, 69, 928-932.	0.4	0
575	ã,»ãf©ãfŸāffā,¯æœ–™ã«ãŠã'ã,‹é«~速è¶åj'性. Materia Japan, 2006, 45, 640-643.	0.1	0
576	Mechanical Properties of Textured Alumina Prepared by Colloidal Processing in a Strong Magnetic Field. Materials Research Society Symposia Proceedings, 2006, 977, 1.	0.1	0

#	Article	IF	CITATIONS
577	Thermoelectric Properties and Magnetic Anisotropies of Magnetically Grain-Oriented Sr- or Bi-doped Ca3Co4O9 Thick Films. Materials Research Society Symposia Proceedings, 2007, 1044, 1.	0.1	0
578	Improvement of Thermoelectric Properties of p- and n-types Oxide Thick Films Fabricated by Electrophoretic Deposition. Materials Research Society Symposia Proceedings, 2007, 1044, 1.	0.1	0
579	Hydrogen Storage Properties of Nb-Zr-Fe Alloys Disintegrated by Hydrogen Gas. Materials Science Forum, 2007, 534-536, 73-76.	0.3	0
580	Preparation and Some Properties of Ni-TiN and Ni-TiC Nanocomposite Particles by DC Arc-Plasma. Key Engineering Materials, 2007, 336-338, 2082-2085.	0.4	0
581	Fabrication of Highly Microstructure Controlled Ceramics by Novel Colloidal Processing. Key Engineering Materials, 0, 336-338, 2372-2377.	0.4	0
582	CONTROL OF NANOSTRUCTURE OF MATERIALS. , 2008, , 177-265.		0
583	Textured PbTiO ₃ Based Ceramics Fabricated by Slip Casting in a High Magnetic Field. Key Engineering Materials, 0, 421-422, 395-398.	0.4	0
584	Fabrication of Multi-Layered Thermoelectric Thick Films and their Thermoelectric Performance. Key Engineering Materials, 2009, 412, 291-296.	0.4	0
585	Elucidation of Crystal-Chemical Determination Factor of Magnetic Anisotropy in HTSC. IEEE Transactions on Applied Superconductivity, 2009, 19, 2965-2969.	1.7	0
586	Control of Texture in Diamagnetic Ceramics by Using a Strong Magnetic Field. Materia Japan, 2009, 48, 321-326.	0.1	0
587	3rd International Workshop on Materials Analysis and Processing in Magnetic Fields (MAP3). Journal of Physics: Conference Series, 2009, 156, 011001.	0.4	0
588	Fabrication of Textured β-Si ₃ N ₄ and β-Sialon by Slip Casting in a Strong Magnetic Field and Reaction-Sintering. Key Engineering Materials, 0, 434-435, 5-8.	0.4	0
589	Microstructure Control of Barium Titanate - Potassium Niobate Solid Solution System Ceramics by MPB Engineering and Their Piezoelectric Properties. IOP Conference Series: Materials Science and Engineering, 2011, 18, 092058.	0.6	0
590	Tailoring Plate-Like Grained ZrB ₂ Ceramic via a Strong Magnetic Field Alignment Method Followed by Spark Plasma Sintering. Key Engineering Materials, 2012, 512-515, 702-705.	0.4	0
591	Controlled Thermal Plasma Processing ofÂCeramic Nanopowders. , 2013, , 979-989.		0
592	Preparation of Barium Titanate Nanoperticles with Necking Structure/Polymer Complex and their Dielectric Properties. Key Engineering Materials, 0, 582, 23-26.	0.4	0
593	Preparation of Ceramics/Polymer Film Capacitor Using Barium Titanate Nanoparticles with High Dielectric Property and their Dielectric Property. Key Engineering Materials, 0, 566, 54-58.	0.4	0
594	Particle processing technology. Science and Technology of Advanced Materials, 2014, 15, 010201.	6.1	0

#	Article	IF	CITATIONS
595	Influence of Loading Condition on Fabrication of Transparent MgAl ₂ O ₄ Spinel Ceramics by Spark-Plasma-Sintering (SPS) Technique. Funtai Oyobi Fummatsu Yakin/Journal of the Japan Society of Powder and Powder Metallurgy, 2014, 61, 565-574.	0.2	0
596	Effects of High Magnetic Fields on Thermal Convection Using Feeble Magnetic Conductive Aqueous Solutions. Bulletin of the Chemical Society of Japan, 2015, 88, 1404-1409.	3.2	0
597	Textured Beta-Sialon:Eu ²⁺ Phosphor Deposits Fabricated by Electrophoretic Deposition (EPD) Process within a Strong Magnetic Field: Preparation Process and Photoluminescence (PL) Properties Depending on Orientation. Key Engineering Materials, 0, 654, 268-273.	0.4	0
598	Fabrication of c-Axis-Oriented Zeolite L Seed Layer on Porous Zirconia Substrate by Electrophoretic Deposition in Strong Magnetic Field. Key Engineering Materials, 0, 654, 274-279.	0.4	0
599	Development of powder processing under external fields. Funtai Oyobi Fummatsu Yakin/Journal of the Japan Society of Powder and Powder Metallurgy, 2016, 63, 793.	0.2	0
600	Preparation of Gallium Stannate Dense Sintered Body Using SPS Method. Funtai Oyobi Fummatsu Yakin/Journal of the Japan Society of Powder and Powder Metallurgy, 2016, 63, 986-989.	0.2	0
601	Fabrication and Mechanical Properties of Textured Ti ₃ SiC ₂ Systems Using Commercial Powders. Funtai Oyobi Fummatsu Yakin/Journal of the Japan Society of Powder and Powder Metallurgy, 2017, 64, 552-557.	0.2	0
602	Possibility of Low-Temperature High-Strain-Rate Superplasticity in Fine-Grained Ceramic Materials. Funtai Oyobi Fummatsu Yakin/Journal of the Japan Society of Powder and Powder Metallurgy, 2017, 64, 515-522.	0.2	0
603	Preparation of Double-shelled Fluorescent Silicon Nanocrystals and Fabrication of Its Thin Layer by Electrophoretic Deposition Process. Funtai Oyobi Fummatsu Yakin/Journal of the Japan Society of Powder and Powder Metallurgy, 2018, 65, 108-113.	0.2	0
604	Fabrication of Ceramics With Highly Controlled Microstructures by Advanced Powder Processing. , 2018, , 801-807.		0
605	Preparation of Double-Shelled Fluorescent Silicon Nanocrystals and Fabrication of Its Thin Layer by Electrophoretic Deposition Process. Materials Transactions, 2019, 60, 49-54.	1.2	0
606	Effect of MgAl2O4 Spinel Dispersion on High-Strain-Rate Superplasticity in Tetragonal ZrO2 Polycrystal. Nippon Kinzoku Gakkaishi/Journal of the Japan Institute of Metals, 2005, 69, 356-361.	0.4	0
607	FABRICATION OF FLUORAPATITE CERAMIC MATERIAL WITH SUBMICROME -45- TER-SIZED GRAINS AND ITS HIGH-TEMPERATURE PLASTIC DEFORMATION. Phosphorus Research Bulletin, 2009, 23, 45-51.	0.6	0
608	Solution Synthesis of Luminescent Silicon Nanoparticles. Journal of the Japan Society of Colour Material, 2009, 82, 516-521.	0.1	0
609	EFFECT OF β-CALCIUM ORTHOPHOSPHATE ADDITION ON HIGH- TEMPERATURE PLASTIC DEFORMATION OF HYDROXYAPATITE WITH SUBMICROMETER-SIZED GRAINS. Phosphorus Research Bulletin, 2012, 27, 11-17.	0.6	0
610	TEM Characterization of Nanocomposite Materials. , 2014, , 333-373.		0
611	Sintering of Copper Ultrafine Powders. , 1989, , 193-202.		0
612	Sinterable Powder Fabrication and the Oxygen-ion Conductivity of Lanthanum Silicate Oxyapatite. Journal of the Society of Powder Technology, Japan, 2015, 52, 648-657.	0.1	0

#	Article	IF	CITATIONS
613	Dense lanthanum silicate oxyapatite ceramics obtained by uniaxial pressing and slip casting. Science of Sintering, 2018, 50, 433-443.	1.4	0
614	High Performance of Ceramics and Manufacturing Process Innovation. Funtai Oyobi Fummatsu Yakin/Journal of the Japan Society of Powder and Powder Metallurgy, 2018, 65, 457.	0.2	0
615	Development of Laser Optical Elements by Spark Plasma Sintering Technique. The Review of Laser Engineering, 2019, 47, 448.	0.0	0
616	New Development of Powder Processing under Eternal Fields. Funtai Oyobi Fummatsu Yakin/Journal of the Japan Society of Powder and Powder Metallurgy, 2020, 67, 47.	0.2	0
617	Fabrication Alumina Film with High Breakdown Field Strength by New Aerosol Gas Deposition Technology. Funtai Oyobi Fummatsu Yakin/Journal of the Japan Society of Powder and Powder Metallurgy, 2020, 67, 220-223.	0.2	0